Author/s:
Saner, FAM;Takahashi, K;Budden, T;Pandey, A;Ariyaratne, D;Zwimpfer, TA;Meagher, NS;Fereday, S;Twomey, L;Pishas, KI;Hoang, T;Bolithon, A;Traficante, N;Alsop, K;Christie, EL;Kang, EY;Nelson, GS;Ghatage, P;Lee, CH;Riggan, MJ;Alsop, J;Beckmann, MW;Boros, J;Brand, AH;Brooks-Wilson, A;Carney, ME;Coulson, P;Courtney-Brooks, M;Cushing-Haugen, KL;Cybulski, C;El-Bahrawy, MA;Elishaev, E;Erber, R;Gayther, SA;Gentry-Maharaj, A;Blake Gilks, C;Harnett, PR;Harris, HR;Hartmann, A;Hein, A;Hendley, J;Hernandez, BY;Jakubowska, A;Jimenez-Linan, M;Jones, ME;Kaufmann, SH;Kennedy, CJ;Kluz, T;Koziak, JM;Kristjansdottir, B;Le, ND;Lener, M;Lester, J;Lubiński, J;Mateoiu, C;Orsulic, S;Ruebner, M;Schoemaker, MJ;Shah, M;Sharma, R;Sherman, ME;Shvetsov, YB;Rinda Soong, T;Steed, H;Sukumvanich, P;Talhouk, A;Taylor, SE;Vierkant, RA;Wang, C;Widschwendter, M;Wilkens, LR;Winham, SJ;Anglesio, MS;Berchuck, A;Brenton, JD;Campbell, I;Cook, LS;Doherty, JA;Fasching, PA;Fortner, RT;Goodman, MT;Gronwald, J;Huntsman, DG;Karlan, BY;Kelemen, LE;Menon, U;Modugno, F;Pharoah, PDP;Schildkraut, JM;Sundfeldt, K;Swerdlow, AJ;Goode, EL;DeFazio, A;Köbel, M;Ramus, SJ;Bowtell, DDL;Garsed, DW

Title:
Concurrent RB1 Loss and BRCA Deficiency Predicts Enhanced Immunologic Response and Long-term Survival in Tubo-ovarian High-grade Serous Carcinoma

Date:
2024-08-15

Citation:
Saner, F. A. M., Takahashi, K., Budden, T., Pandey, A., Ariyaratne, D., Zwimpfer, T. A., Meagher, N. S., Fereday, S., Twomey, L., Pishas, K. I., Hoang, T., Bolithon, A., Traficante, N., Alsop, K., Christie, E. L., Kang, E. Y., Nelson, G. S., Ghatage, P., Lee, C. H. ,... Garsed, D. W. (2024). Concurrent RB1 Loss and BRCA Deficiency Predicts Enhanced Immunologic Response and Long-term Survival in Tubo-ovarian High-grade Serous Carcinoma. Clinical Cancer Research, 30 (16), pp.3481-3498. https://doi.org/10.1158/1078-0432.CCR-23-3552.

Persistent Link:
https://hdl.handle.net/11343/351505

Concurrent RB1 Loss and *BRCA*-Deficiency Predicts Enhanced Immunological Response and Long-Term Survival in Tubo-Ovarian High-Grade Serous Carcinoma

Flurina A. M. Saner[1,2,†], Kazuaki Takahashi[1,3,†], Timothy Budden[4,5], Ahwan Pandey[1], Dinuka Ariyaratne[1], Tibor A. Zwimpfer[1], Nicola S. Meagher[4,6], Sian Fereday[1,7], Laura Twomey[1], Kathleen I. Pishas[1,7], Therese Hoang[1], Adelyn Bolithon[4,8]; Nadia Traficante[1,7], for the Australian Ovarian Cancer Study Group; Kathryn Alsop[1,7], Elizabeth L. Christie[1,7], Eun-Young Kang[9], Gregg S. Nelson[10], Prafull Ghatage[10], Cheng-Han Lee[11], Marjorie J. Riggan[12], Jennifer Alsop[13], Matthias W. Beckmann[14], Jessica Boros[15-17], Alison H. Brand[16,17], Angela Brooks-Wilson[18], Michael E. Carney[19], Penny Coulson[20], Madeleine Courtney-Brooks[21], Kara L. Cushing-Haugen[22], Cezary Cybulski[23], Mona A. El-Bahrawy[24], Esther Elishaev[25], Ramona Erber[26], Simon A. Gayther[27], Aleksandra Gentry-Maharaj[28,29], C. Blake Gilks[30], Paul R. Harnett[17,31], Holly R. Harris[22,32], Arndt Hartmann[26], Alexander Hein[14], Joy Hendley[1], Brenda Y. Hernandez[33], Anna Jakubowska[23,34], Mercedes Jimenez-Linan[35], Michael E. Jones[20], Scott H. Kaufmann[36], Catherine J. Kennedy[15,17], Tomasz Kluz[37], Jennifer M. Koziak[38], Björg Kristjansdottir[39], Nhu D. Le[40], Marcin Lener[41], Jenny Lester[42], Jan Lubiński[23], Constantina Mateoiu[43], Sandra Orsulic[42], Matthias Ruebner[14], Minouk J. Schoemaker[21], Mitul Shah[13], Raghwa Sharma[44], Mark E. Sherman[45], Yurii B. Shvetsov[34], T. Rinda Soong[25], Helen Steed[46,47], Paniti Sukumvanich[21], Aline Talhouk[48,49], Sarah E. Taylor[21], Robert A. Vierkant[50], Chen Wang[51], Martin Widschwendter[52], Lynne R. Wilkens[34], Stacey J. Winham[51], Michael S. Anglesio[48,49], Andrew Berchuck[12], James D. Brenton[53], Ian Campbell[1,7], Linda S. Cook[54,55], Jennifer A. Doherty[56], Peter A. Fasching[14], Renée Turzanski Fortner[57,58], Marc T. Goodman[59], Jacek Gronwald[23], David G. Huntsman[30,48,49,60], Beth Y. Karlan[42], Linda E. Kelemen[61], Usha Menon[28], Francesmary Modugno[21,62,63] Paul D.P. Pharoah[13,64,65], Joellen M. Schildkraut[66], Karin Sundfeldt[40], Anthony J. Swerdlow[20,67], Ellen

L. Goode[68], Anna DeFazio[6,15-17], Martin Köbel[9,‡], Susan J. Ramus[4,8,‡], David D. L. Bowtell[1,7,‡], and Dale W. Garsed[1,7,‡,*]

[1]Peter MacCallum Cancer Centre, Melbourne, Victoria, Australia.

[2]Department of Obstetrics and Gynecology, Bern University Hospital and University of Bern, Bern, Switzerland.

[3]Department of Obstetrics and Gynecology, The Jikei University School of Medicine, Tokyo, Japan.

[4]School of Clinical Medicine, UNSW Medicine and Health, University of NSW Sydney, Sydney, New South Wales, Australia.

[5]Skin Cancer and Ageing Lab, Cancer Research United Kingdom Manchester Institute, The University of Manchester, Manchester, UK.

[6]The Daffodil Centre, The University of Sydney, a joint venture with Cancer Council NSW, Sydney, New South Wales, Australia.

[7]Sir Peter MacCallum Department of Oncology, The University of Melbourne, Parkville, Victoria, Australia.

[8]Adult Cancer Program, Lowy Cancer Research Centre, University of NSW Sydney, Sydney, New South Wales, Australia.

[9]Department of Pathology and Laboratory Medicine, University of Calgary, Foothills Medical Center, Calgary, AB, Canada.

[10]Department of Oncology, Division of Gynecologic Oncology, Cumming School of Medicine, University of Calgary, Calgary, AB, Canada.

[11]Department of Laboratory Medicine and Pathology, University of Alberta, Edmonton, Alberta, Canada.

[12]Department of Obstetrics and Gynecology, Division of Gynecologic Oncology, Duke University Medical Center, Durham, NC, USA.

[13]Centre for Cancer Genetic Epidemiology, Department of Oncology, University of Cambridge, Cambridge, UK.

[14]Department of Gynecology and Obstetrics, Comprehensive Cancer Center Erlangen-EMN, Friedrich-Alexander University Erlangen-Nuremberg, University Hospital Erlangen, Erlangen, Germany.

[15]Centre for Cancer Research, The Westmead Institute for Medical Research, Sydney, New South Wales, Australia.

[16]Department of Gynaecological Oncology, Westmead Hospital, Sydney, New South Wales, Australia.

[17]The University of Sydney, Sydney, New South Wales, Australia.

[18]Canada's Michael Smith Genome Sciences Centre, BC Cancer, Vancouver, BC, Canada.

[19]Department of Obstetrics and Gynecology, John A. Burns School of Medicine, University of Hawaii, Honolulu, HI, USA.

[20]Division of Genetics and Epidemiology, The Institute of Cancer Research, London, UK.

[21]Department of Obstetrics, Gynecology and Reproductive Sciences, University of Pittsburgh School of Medicine, Pittsburgh, PA, USA.

[22]Program in Epidemiology, Division of Public Health Sciences, Fred Hutchinson Cancer Center, Seattle, WA, USA.

[23]Department of Genetics and Pathology, International Hereditary Cancer Center, Pomeranian Medical University, Szczecin, Poland.

[24]Department of Metabolism, Digestion and Reproduction, Imperial College London, Hammersmith Hospital, London, UK.

[25]Department of Pathology, University of Pittsburgh School of Medicine, Pittsburgh, PA, USA.

[26]Institute of Pathology, Comprehensive Cancer Center Erlangen-EMN, Friedrich-Alexander University Erlangen-Nuremberg, University Hospital Erlangen, Erlangen, Germany.

[27]Center for Bioinformatics and Functional Genomics and the Cedars Sinai Genomics Core, Cedars-Sinai Medical Center, Los Angeles, CA, USA.

[28]MRC Clinical Trials Unit, Institute of Clinical Trials and Methodology, University College London, London, UK.

[29]Department of Women's Cancer, Elizabeth Garrett Anderson Institute for Women's Health, University College London, London, UK

[30]Department of Pathology and Laboratory Medicine, University of British Columbia, Vancouver, BC, Canada.

[31]Crown Princess Mary Cancer Centre, Westmead Hospital, Sydney, New South Wales, Australia.

[32]Department of Epidemiology, University of Washington, Seattle, WA, USA.

[33]University of Hawaii Cancer Center, Honolulu, HI, USA.

[34]Independent Laboratory of Molecular Biology and Genetic Diagnostics, Pomeranian Medical University, Szczecin, Poland.

[35]Department of Histopathology, Addenbrooke's Hospital, Cambridge, UK.

[36]Division of Oncology Research, Department of Oncology, Mayo Clinic, Rochester, MN, USA.

[37]Department of Gynecology and Obstetrics, Gynecology Oncology and Obstetrics, Institute of Medical Sciences, Medical College of Rzeszow University, Rzeszów, Poland.

[38]Alberta Health Services-Cancer Care, Calgary, AB, Canada.

[39]Department of Obstetrics and Gynecology, Institute of Clinical Sciences, Sahlgrenska Center for Cancer Research, University of Gothenburg, Gothenburg, Sweden.

[40]Cancer Control Research, BC Cancer Agency, Vancouver, BC, Canada.

[41]International Hereditary Cancer Center, Department of Genetics and Pathology, Pomeranian Medical University in Szczecin, Szczecin, Poland.

[42]David Geffen School of Medicine, Department of Obstetrics and Gynecology, University of California at Los Angeles, Los Angeles, CA, USA.

[43]Department of Pathology, University of Gothenburg, Gothenburg, Sweden.

[44]Tissue Pathology and Diagnostic Oncology, Westmead Hospital, Sydney, New South Wales, Australia.

[45]Department of Health Sciences Research, Mayo Clinic, Jacksonville, FL, USA.

[46]Division of Gynecologic Oncology, Department of Obstetrics and Gynecology, University of Alberta, Edmonton, Alberta, Canada.

[47]Section of Gynecologic Oncology Surgery, North Zone, Alberta Health Services, Edmonton, Alberta, Canada.

[48]British Columbia's Gynecological Cancer Research Team (OVCARE), University of British Columbia, BC Cancer, and Vancouver General Hospital, Vancouver, BC, Canada.

[49]Department of Obstetrics and Gynecology, University of British Columbia, Vancouver, BC, Canada.

[50]Department of Quantitative Health Sciences, Division of Clinical Trials and Biostatistics, Mayo Clinic, Rochester, MN, USA.

[51]Department of Quantitative Health Sciences, Division of Computational Biology, Mayo Clinic, Rochester, MN, USA.

[52]EUTOPS Institute, University of Innsbruck, Innsbruck, Austria.

[53]Cancer Research UK Cambridge Institute, University of Cambridge, Cambridge, UK.

[54]Epidemiology, School of Public Health, University of Colorado, Aurora, CO, USA.

[55]Community Health Sciences, University of Calgary, Calgary, AB, Canada.

[56]Huntsman Cancer Institute, Department of Population Health Sciences, University of Utah, Salt Lake City, UT, USA.

[57]Division of Cancer Epidemiology, German Cancer Research Center (DKFZ), Heidelberg, Germany.

[58]Department of Research, Cancer Registry of Norway, Norwegian Institute of Public Health, Oslo, Norway.

[59]Cancer Prevention and Control Program, Cedars-Sinai Cancer, Cedars-Sinai Medical Center, Los Angeles, CA, USA.

[60]Department of Molecular Oncology, BC Cancer Research Centre, Vancouver, BC, Canada.

[61]Division of Acute Disease Epidemiology, South Carolina Department of Health & Environmental Control, Columbia, SC, USA.

[62]Department of Epidemiology, University of Pittsburgh School of Public Health, Pittsburgh, PA, USA.

[63]Women's Cancer Research Center, Magee-Womens Research Institute and Hillman Cancer Center, Pittsburgh, PA, USA.

[64]Department of Computational Biomedicine, Cedars-Sinai Medical Center, West Hollywood, CA, USA.

[65]Centre for Cancer Genetic Epidemiology, Department of Public Health and Primary Care, University of Cambridge, Cambridge, UK.

[66]Department of Epidemiology, Rollins School of Public Health, Emory University, Atlanta, GA, USA.

[67]Division of Breast Cancer Research, The Institute of Cancer Research, London, UK.

[68]Department of Quantitative Health Sciences, Division of Epidemiology, Mayo Clinic, Rochester, MN, USA.

[†]These authors contributed equally to the work.

[‡]These authors contributed equally to the work.

Running title:

RB1 Loss and Survival in Ovarian Carcinoma

*Correspondence to: Dr Dale W. Garsed, Peter MacCallum Cancer Centre, 305 Grattan St, Melbourne, 3000, Australia, Dale.Garsed@petermac.org

Author's Disclosures

DDLB is an Exo Therapeutics advisor and has received research grant funding from AstraZeneca, Genentech-Roche and BeiGene for unrelated work. SF, NT, KA, and ADeF received grant funding from AstraZeneca for unrelated work. AGM and UM report funded research collaborations for unrelated work with industry: Intelligent Lab on Fiber, RNA Guardian, Micronoma and Mercy BioAnalytics. UM had stock ownership (2011-2021) awarded by University College London (UCL) in Abcodia, which held the license for the Risk of Ovarian Cancer Algorithm (ROCA). UM reports research collaboration contracts with Cambridge University and QIMR Berghofer Medical Research Institute. UM holds patent number EP10178345.4 for Breast Cancer Diagnostics. UM is a member of Tina's Wish Scientific Advisory Board (USA) and Research Advisory Panel, Yorkshire Cancer Research (UK). Dr. Köbel reports personal fees from Helix Biopharma outside the submitted work. The remaining authors declared no conflicts of interest.

Translational Relevance

Improved understanding of the gene alterations associated with homologous recombination deficiency (HRD) and drug sensitivity will enable better prognostication and treatment stratification in patients with HRD-prone cancers. In a large cohort of 7,436 patients with ovarian carcinoma, we found that tumor RB1 protein loss was most frequent (16.4%) in tubo-ovarian high-grade serous carcinoma (HGSC) and associated with longer overall survival (OS). The positive effect of RB1 loss on survival was more pronounced in patients with co-occurring HRD gene alterations; most frequently germline *BRCA1* or *BRCA2* (*BRCA*) pathogenic variants. In contrast, patients with combined RB1 loss and homologous recombination proficiency exhibit a worse prognosis, suggesting the relationship between RB1 loss and survival is HRD-dependent. RB1 expression is assessable by an affordable and accessible immunohistochemistry assay and could be considered as a stratification factor, along with HRD tests, in future trials to determine whether it's predictive of response to chemotherapy and/or PARP inhibitors.

Abstract

Purpose: To evaluate RB1 expression and survival across ovarian carcinoma histotypes, and how co-occurrence of *BRCA1* or *BRCA2* (*BRCA*) alterations and RB1 loss influences survival in tubo-ovarian high-grade serous carcinoma (HGSC).

Experimental Design: RB1 protein expression was classified by immunohistochemistry in ovarian carcinomas of 7436 patients from the Ovarian Tumor Tissue Analysis consortium. We examined RB1 expression and germline *BRCA* status in a subset of 1134 HGSC, and related genotype to overall survival (OS), tumor-infiltrating CD8+ lymphocytes and transcriptomic subtypes. Using CRISPR-Cas9, we deleted *RB1* in HGSC

cells with and without *BRCA1* alterations to model co-loss with treatment response. We performed whole-genome and transcriptome data analyses on 126 primary HGSC to characterize tumors with concurrent *BRCA*-deficiency and *RB1* loss.

Results: RB1 loss was associated with longer OS in HGSC, but with poorer prognosis in endometrioid ovarian carcinoma. Patients with HGSC harboring both RB1 loss and pathogenic germline *BRCA* variants had superior OS compared to patients with either alteration alone, and their median OS was three times longer than those without pathogenic *BRCA* variants and retained RB1 expression (9.3 vs. 3.1 years). Enhanced sensitivity to cisplatin and paclitaxel was seen in *BRCA1*-altered cells with *RB1* knockout. Combined *RB1* loss and *BRCA*-deficiency correlated with transcriptional markers of enhanced interferon response, cell-cycle deregulation, and reduced epithelial-mesenchymal transition. CD8+ lymphocytes were most prevalent in *BRCA*-deficient HGSC with co-loss of *RB1*.

Conclusions: Co-occurrence of RB1 loss and *BRCA*-deficiency was associated with exceptionally long survival in patients with HGSC, potentially due to better treatment response and immune stimulation.

Introduction

Despite a high response rate to primary treatment, the progressive development of acquired drug resistance is common in tubo-ovarian high-grade serous carcinoma (HGSC), a histotype that is associated with approximately 70% of ovarian cancer deaths (1). The frequent acquisition of resistance-conferring alterations in HGSC (2-4) suggests that the development of drug resistance may be inevitable when curative surgery is not achieved in these patients. Countering that view, however, is the observation that a small subset of patients with HGSC advanced disease experience an exceptional response to treatment, survive well beyond a median of 3.4 years (5), and in some cases, remain disease free (6,7).

Interest in studying long-term cancer survivors is growing as they may assist the discovery of prognostic biomarkers, novel treatments, and approaches to limit the development of resistance (8,9).

Several clinical and molecular factors that influence treatment response and overall survival (OS) in HGSC have been described. Complete surgical debulking is associated with a more favorable outcome compared to patients left with residual disease (10-12). Molecular subtypes defined by distinct gene expression patterns in primary HGSC are associated with different outcomes (13), including the poor survival C1/mesenchymal subtype that is more often seen in patients where complete surgical tumor resection cannot be achieved (14-16). By contrast, the C2/immunoreactive subtype is typified by extensive infiltration of intraepithelial T cells (13), a feature known to be strongly associated with improved survival (17,18). Tumors arising in individuals with germline or somatic alterations in *BRCA1* or *BRCA2* genes are typically more responsive to conventional chemotherapy and poly(ADP-ribose) polymerase (PARP) inhibitors, whereas those tumors with intact homologous recombination (HR) DNA repair are more often resistant to treatment (19-21). Patients with germline *BRCA1* or *BRCA2* pathogenic variants (g*BRCA*var) show more favorable survival at five years post-diagnosis compared to those with wild-type germline *BRCA* genes (g*BRCA*wt), and those with germline *BRCA2* pathogenic variants retain a long-term (>10 year) survival advantage (22-24). Although deleterious alterations in *BRCA1*, *BRCA2* and other genes involved in HR DNA repair are associated with a favorable response to treatment, these are not sufficient alone to confer long-term survival and a large proportion of such patients experience a typical disease trajectory. Differential outcomes in *BRCA*-driven HGSC can in part be ascribed to alternative splicing (25), retention of the wild-type *BRCA* allele in tumors (26), or the acquisition of reversion mutations (2,3), all of which appear to limit the effectiveness of chemotherapy.

We previously characterized a small series of HGSC exceptional survivors and found that co-occurring loss of function alterations in both *BRCA* and *RB1* were associated with unusually favorable survival (7,27). Disruption of the RB pathway is found in many cancer types but with variable impacts on patient outcome. For example, co-loss of *RB1* and *BRCA* is associated with shorter survival in breast and prostate cancer, possibly due to lineage switching and resistance to hormonal therapy (28-30). A transcriptomic signature of RB1 loss was recently described to be associated with poor outcomes across cancer types (31). We have previously found that chromosomal breakage is the most common mechanism of *RB1* inactivation in HGSC (3), accounting for approximately 80% of all *RB1* alterations. In addition to its crucial role in cell cycle regulation, RB1 is involved in non-canonical functions in a context- and tissue-dependent manner (32-34), including HR mediated DNA repair. Loss of RB1 expression in HGSC has been associated with a survival benefit (35), including in the context of abnormal block-like p16 staining (36).

Factors underlying the association of RB1 loss with improved outcome in HGSC are unknown. Here, we contrast the pattern and clinical consequences of RB1 loss in HGSC with other epithelial ovarian cancer subtypes, investigate the relevance of co-occurring *BRCA1* or *BRCA2* alterations and RB1 loss in patients with HGSC, and explore the functional effects of combined *BRCA* and *RB1* impairment in HGSC cell lines.

Materials and Methods

Patient cohorts

The study population consisted of 7436 patients diagnosed with invasive epithelial ovarian, peritoneal or fallopian tube cancer from 20 studies or biobanks participating in the Ovarian Tumor Tissue Analysis (OTTA) consortium (37) (Table 1, Supplementary Fig. S1). This study was conducted in accordance with the principles of Good Clinical Practice and the

Declaration of Helsinki. Written informed consent or an institutional review board approved waiver of consent was obtained at each site for patient recruitment, sample collection, and study protocols (Supplementary Table S1). Human investigations were performed after approval by local human research ethics committees/institutional review boards at each site and in accordance with an assurance filed with and approved by the U.S. Department of Health and Human Services, where appropriate. Cases in this study were recruited before the widespread use of *BRCA* testing and PARP inhibitors (median year of diagnosis 2004, 25-75% quartiles 2001-2007, 5-95% percentiles 1993-2012, range 1978-2016).

Whole-genome sequence and matched transcriptome sequence data of primary HGSC tumors were available from 126 patients from the Multidisciplinary Ovarian Cancer Outcomes Group (MOCOG) study (27) (Supplementary Fig. S1). This cohort consisted of 34 short-term survivors (OS <2 years), 32 moderate-term survivors (OS ≥2 and <10 years) and 60 long-term survivors (OS ≥10 years) with advanced stage (IIIC/IV) disease, enrolled in the Australian Ovarian Cancer Study (AOCS), the Gynaecological Oncology Biobank at Westmead Hospital (Sydney) or the Mayo Clinic Study.

Immunohistochemical (IHC) staining and analysis of RB1 protein expression

RB1 protein expression was determined by IHC staining and scoring of tissue microarrays (TMAs) from formalin-fixed paraffin-embedded (FFPE) tumor samples, using our previously described protocol (7). Sections of 4 μm thickness of previously constructed TMAs, with each case represented by 1-3 cores (either 0.6 mm, 1 mm, or 2 mm in diameter), were shipped to a central IHC laboratory at the University of Calgary (Alberta, Canada). Detailed information on the anatomical site of the tissue microarray source is not available for every sample, however, for the OTTA studies where this information is available, most cases (86%) were sampled from the adnexal tubo-ovarian tumor. FFPE samples on slides

were subjected to heat induced antigen retrieval with Target Retrieval Solution (TRS) high on the DAKO Omnis platform (Agilent Technologies, Santa Clara, CA, USA), then incubated with anti-RB1 (Retinoblastoma Gene Protein) mouse monoclonal antibody (Leica, Clone 13A10, Novocastra: #NCL-L-RB-358) at a 1:100 dilution. Staining was visualized using 3,3'-diaminobenzidine (DAB).

Samples were scored as either 0 (absent RB1 expression with RB1 expression present in normal cells serving as internal control), 1 (RB1 present), 2 (subclonal loss of RB1 expression), 3 (cytoplasmic staining) or uninterpretable, which was scored as either 8 (RB1 absent but lacking adjacent internal control) or 9 (sample drop out). Representative images of RB1 expression patterns in tumor tissue are shown in Supplementary Fig. S2. Scoring was conducted by two pathologists (MK and EYK). Using two test TMAs with 192 cores, the interobserver agreement was 89.9% (kappa=0.816), including the assessment of whether the core was interpretable. When considering only the 156 cores that both pathologists deemed interpretable, the interobserver agreement was 98.1% (kappa=0.92).

Molecular analyses

Subsets of patients with HGSC had additional molecular or immune data available (Supplementary Fig. S1), including tumor p53 protein expression status previously classified (38) as normal (wild-type) or abnormal (overexpression, complete absence, and cytoplasmic), germline *BRCA1* and *BRCA2* pathogenic variant status obtained from OTTA, *RB1* mRNA tumor expression and transcriptional subtypes of tumors using NanoString (35,39), and CD8+ tumor infiltrating lymphocyte (TIL) density was previously classified (40) based on the number of CD8+ TILs per high-powered field: negative (no TILs), low (<3 TILs), moderate (3-19 TILs) or high (≥20 TILs).

The MOCOG whole-genome and transcriptome sequencing dataset of 126 short-, moderate- and long-term survivors was uniformly processed as previously described (27), and included detailed characterization of each tumor sample for inactivating alterations in *RB1* and HR pathway genes, including germline and/or somatic genetic alterations in *BRCA1*, *BRCA2*, *BRIP1*, *PALB2*, *RAD51C* and *RAD51D*, or promoter methylation of *BRCA1* and *RAD51C*. Homologous recombination deficiency (HRD) status was assessed using the CHORD (Classifier of Homologous Recombination Deficiency) method (41), which uses specific base substitution, indel and structural rearrangement signatures detected in tumor genomes to generate *BRCA1*-type and *BRCA2*-type HRD scores. Primary tumors were classified as either *BRCA1*-HRD & *RB1* altered; *BRCA1*-HRD & *RB1* wild-type; *BRCA2*-HRD & *RB1* altered; *BRCA2*-HRD & *RB1* wild-type; homologous recombination proficient (HRP) & *RB1* altered, or HRP & *RB1* wild-type.

RNA-sequencing normalization and batch correction

Primary high-grade serous tubo-ovarian carcinoma (HGSC) samples were grouped according to *RB1* alterations and homologous recombination deficiency (HRD) status, as assessed previously using whole-genome sequencing (27) and the CHORD (Classifier of Homologous Recombination Deficiency) method (41) (Supplementary Table S2). Matched RNA sequencing data was previously processed into gene expression counts as part of the prior MOCOG study (27). Briefly, raw counts data was filtered to include only protein coding genes. Lowly expressed genes were removed by converting the data to CPM (counts per million = number of reads mapped to a gene x 10^6 / total number of mapped reads) and only genes where at least 10 samples had a CPM of greater than 0.5 were kept for further processing. The data was TMM normalized using edgeR (RRID:SCR_012802) and batch effects removed using the removeBatchEffect function of limma (RRID:SCR_010943). The

batch correction was performed to remove batch effects while retaining group differences using limma's removeBatchEffect function with the parameters (exp_data, batch = LibraryType, design = model.matrix(~HR_RB1_status)) where "exp_data" is the $\log_2$ TMM normalized data. The design of the study is shown in Supplementary Table S3.

Differential gene expression analysis

Differentially expressed protein coding genes were identified between sample groups of interest using DESeq2 (RRID:SCR_015687) (42) (v1.26.0), with batch effects accounted for in the model. In addition to characterizing the transcriptional profiles of tumors with *RB1* alterations and concomitant *BRCA1*- or *BRCA2*-type HRD relative to tumors with no alterations, DESeq2 was also used to evaluate alteration-specific transcriptional profiles by incorporating given alterations into the model to remove their signal (each comparison is shown in Supplementary Table S4). *HLA* associated genes present in the differential expression results from DESeq2 were annotated to their relevant classes (43).

The R package FGSEA (fast gene set enrichment analysis; v1.15.1; bioRxiv https://doi.org/10.1101/060012) was used to perform gene set enrichment analyses across comparison groups. Gene level Benjamini-Hochberg adjusted *P* values obtained from DESeq2 were transformed to signed *P* values by converting them to a negative log10 value and applying the sign of the fold change. The signed *P* values were pre-sorted and fed into FGSEA via its function fgseaMultilevel (minSize=15, maxSize = 500, gseaParam = 0, eps = 0) to generate enrichment scores and adjusted *P* values using the MSigDB (44) Hallmark gene sets (v7.4).

Gene set variation analysis (GSVA) pathway enrichment

Gene lists for the cGAS-STING and Toll-like receptor signaling pathways were obtained from the PathCards database (45). Gene set enrichment was performed between the normalized batch corrected expression matrix and the pathways using the GSVA R package (v1.34.0) with parameters (method="gsva", kcdf = "Gaussian", min.sz = 5, max.sz = 500).

Cell culture

The AOCS patient-derived cell lines (AOCS1, AOCS3, AOCS7.2 AOCS9, AOCS11.2, AOCS14, AOCS16, AOCS22, AOCS30) were established from ascites drained from patients with HGSC, as previously described (46). All AOCS cell lines were authenticated against matched patient germline DNA using short tandem repeat markers (STR, GenePrint10 System, Promega). Commercial cell lines OAW28 and CAOV3, categorized as likely HGSC(47), were purchased from the American Type Culture Collection (ATCC). Commercial lines were authenticated by comparing STR profiles (GenePrint10 System, Promega) to those published by online repositories (Cancer Cell Line Encyclopedia (48), The cBio Cancer Genomics Portal (49)) before use in experiments. Cell lines were confirmed to be free of *Mycoplasma* by PCR at each revival and after finishing experiments. Cell lines were maintained in a humidified incubator at 37°C and 5% CO_2. All cell lines (aside from OAW28 and CAOV3) were cultured in RPMI 1640 (GIBCO, Carlsbad, CA, USA) supplemented with 10% fetal bovine serum (FBS, Cytiva) and 1% penicillin-streptomycin-glutamine (GIBCO; Supplementary Table S5). OAW28 and CAOV3 were cultured in DMEM (GIBCO) supplemented with 10% FBS and 1% penicillin-streptomycin-glutamine, with the addition of 1mM sodium pyruvate and 20IU/l insulin for OAW28.

Molecular characterization of cell lines

Complete cell line characterization details can be found in Supplementary Table S5 and Supplementary Table S6. The alteration status of genes of interest in AOCS cell lines was determined by either whole-genome (27) or targeted sequencing (7,50) using established pipelines, and in commercial cell lines from published data (47) or The Cancer Cell Line Encyclopedia in cBioPortal (49,51,52). *BRCA* and *TP53* variants were classified as pathogenic if they were truncating (nonsense, splice site or frameshift) alterations resulting in early stop codons, or missense variants previously reported as pathogenic in ClinVar (53) or The TP53 Database (R20, July 2019, https://tp53.isb-cgc.org). *CCNE1* copy number in AOCS cell lines was analyzed by qPCR in triplicate on LightCycler 480 (Roche) using SYBR Green PCR mix (Applied Biosystems) as described previously (54). The expression status of RB1 and p16 was evaluated by Western blot (as below) and/or IHC. For IHC, FFPE cell line plugs were established by fixing approximately $6x10^7$ cells in 10% Neutral Buffered Formalin (NBF) overnight, transferring them into an agarose gel plug and embedding them in paraffin. Duplicate cores were taken from each cell line plug and assembled in a paraffin block in the fashion of a tissue microarray. Cell line microarrays were sectioned, stained with antibodies (RB1, BD Pharmingen, BD Biosciences, clone G3-245; p16, Roche Ventana, CINtec, clone E6H4) and scored blinded by a pathologist. RB1 was classified as either absent, present or uninterpretable; p16 was interpreted according to a 3-tier scoring system as normal patchy, abnormal absent or abnormal overexpressed.

CRISPR-mediated gene knockout

RB1 was inactivated using CRISPR-Cas9 (55) in cell lines with a pre-existing *BRCA1* alteration (AOCS7.2, AOCS16) and a *BRCA1/2* wild-type cell line (AOCS1). Briefly, lentiviral transduction was performed using the FgH1t vector co-expressing Cas9, mCherry, and GFP and a doxycycline inducible synthetic guide RNA (sgRNAs) targeting *RB1* exon 7

or exon 8 (Supplementary Table S7). After sorting for double positive cells (mCherry and GFP) by flow cytometry, expression of the sgRNA was induced with doxycycline (0.1μg/ml media, Sigma-Aldrich, D3072) for 96 hours, and single cells sorted into 96-well plates. Clones were expanded and *RB1* status confirmed by reduced/absent RB1 expression (Western blot, RT-qPCR) and Sanger sequencing of the targeted *RB1* exon. For control lines, *RB1* wild-type single cell colonies without a CRISPR-edit were used, as well as heterogeneous cell populations with transduced Cas9 and sgRNA of a scrambled DNA sequence (56) (Supplementary Table S7).

Dual gene knockout of *RB1* and *BRCA1* was performed in AOCS30 using nucleofection (57-59) rather than lentivirus transduction. *BRCA1*, *RB1*, and control sgRNA sequences (CRISPRevolution sgRNA EZ Kit, Synthego) were designed as previously described (60,61). Cells ($5x10^5$) were trypsinized, washed twice with Phosphate Buffered Saline (PBS) and incubated with the RNP complex (Alt-R® S.p. Cas9 Nuclease purified Cas9 protein, Integrated DNA Technologies) for 10 minutes. Cell pellets were suspended with NucleofectorTM SE solution (Lonza Bioscience) and mixed with prepared Cas9/sgRNA RNP complex, which were transferred into the NucleocuvetteTM vessels (Lonza Bioscience). Nucleofection was conducted with CL-120 Program in 4D-Nucleofector X unit (Lonza Bioscience). Pre-warmed medium was added to cells and incubated for 10 minutes in a humidified 37°C incubator with 5% CO_2. Cells were transferred into 6-well plates and cultured. Each cell line (AOCS30 NT, AOCS30 *BRCA1*KO, AOCS30 *RB1*KO, AOCS30 *RB1BRCA1*KO) was passaged two times to expand following nucleofection, passed through a cell strainer (Falcon 40μm) and plated at a low density (approximately 400 cells per 10cm dish). After ~14 days, independent colonies were trypsinized with cloning discs (Sigma-Aldrich) and expanded. Knockdown efficiency was tested by qPCR as described below.

Western blot analysis

Cells were washed with cold PBS and lysed in 1% SDS (sodium dodecyl sulphate) protein lysis buffer, with addition of proteinase inhibitor and PhosStop solution (Roche) for phosphorylated protein. Protein concentrations were measured using Bio-Rad DC (detergent compatible) protein assay and 40 µg protein in SDS sample buffer and 2-Mercaptoethanol was applied to Mini-PROTEIN TGX Gels 4-20% (Bio-Rad, Hercules, CA, USA), subjected to gel electrophoresis at 115V for 1 hour and 150V for 10 minutes, transferred and blotted to PVDF membranes for 10 minutes at 25V with Trans-Blot Turbo Transfer System (Bio-Rad). Membranes were blocked with Odyssey Blocking Buffer (TBS; LI-COR Bioscience) for 1 hour at room temperature and incubated with the primary antibody (1:500-1:1000 in TBS-T, Supplementary Table S8) overnight at 4°C. After washing the membranes for 3x10 minutes they were incubated with the secondary goat anti-mouse or goat anti-rabbit AB coupled infrared (IR) dye 680 RD or 800 CW (LI-COR, 1:10,000) for 1 hour and, after another 3 washing steps, membranes were imaged using the Odyssey Imaging System (LI-COR).

RNA extraction and qPCR

Total RNA was extracted from cells using RNeasy Kits (QIAGEN) with on-column DNase digestion, of which 1 µg was reverse transcribed into cDNA using the SensiFAST cDNA Synthesis Kit (Meridian Bioscience). Transcript abundance was measured by real-time quantitative PCR (qPCR) using the SYBR Green qPCR assay (Applied Biosystems) on the LightCycler 480 (Roche), with each PCR performed in triplicate. Primer sequences are listed in Supplementary Table S9. Gene expression was estimated using the comparative threshold cycle method (62) (delta-delta Ct) against the average Ct value obtained for two control genes (*GAPDH* and *HPRT*).

Cell viability assay

Cells were seeded at a density of 1 to $8x10^3$ per well, depending on growth rates, in 384-well microtiter plates (Corning®) and incubated overnight. Cisplatin (100 µM; Selleck Chemicals) and olaparib (80 µM, Selleck Chemicals) were diluted in 3-fold steps to create a 10-point dose curve; paclitaxel (0.3 µM, Selleck Chemicals) was diluted in 4-fold steps to create a 12-point dose curve. Following 72 hr (cisplatin and paclitaxel) or 120 hr incubation (olaparib), cells were fixed in 2% paraformaldehyde for 10 minutes, washed with PBS and stained with 0.19% Triton X solution containing DAPI (1:1000; Sigma-Aldrich). Cell dispensing, media changes, and fixing and staining of cells were conducted robotically (BioTek Instruments, Winooski, VT, USA). Drug dispensing was performed with ALH3000 Liquid Handler (PerkinElmer, Waltham, MA, USA). To assess cell viability, the whole area of each well was captured at 10x magnification with CX7-LZR instrument (Thermo Fisher Scientific), and images analyzed with CellProfiler v3.0 pipeline (RRID:SCR_007358). Low quality out-of-focus images (4% of total images) were excluded by manual review before downstream analysis. Non-linear regression drug curves were calculated using GraphPad Prism version 9.3.1 (RRID:SCR_002798) and differences in IC_{50} values statistically measured by applying Akaike's Information Criterion (AIC). Curve fit was compared between *RB1* WT and *RB1* KO clones by an extra sum-of-squares F test.

Clonogenic survival assay

Cells (0.8 to $3x10^3$) were seeded in 6-well plates (Corning®) depending on cell doubling rates. After 12 hours, duplicate wells were treated with cisplatin, paclitaxel or a combination of both drugs at the respective IC_{50} drug concentration, as determined by the 72-hour viability assay. Cells treated with media alone and with DMF solvent containing media served as controls. After 16 days, cells were rinsed with PBS, fixed and stained with 0.1%

crystal violet and methanol for 20 minutes. The whole area of wells was captured in bright-field at 2x magnification using the CX7 (Thermo Fisher Scientific) and the number of clones assessed with the CellProfiler v3.0 software.

Cell proliferation rates

Cells were counted using the Countess 3 Automated Cell Counter (Thermo Fisher Scientific) and seeded in 200 µl media in 96-well Corning® plates in triplicate wells and incubated at 37°C. Cells were plated at three different densities (AOCS1 $6x10^3$ to $8x10^3$ cells/well, AOCS7.2 8 to $12x10^3$ cells/well; AOCS16 14 to $18x10^3$ cells/well) according to a previously observed 20% cell confluency per well on day 1, and media changed after 5 days. The whole well area was captured in brightfield every 12 hours for 9 days using real-live cell imaging (Incucyte® Zoom) and cell proliferation rates determined with Incucyte® software. Growth rates were analyzed separately in triplicate wells with a starting confluency of between 15% and 25% in three independent experiments.

Cell cycle profiling

Cells were seeded in 12-well Corning® plates at between 8 to $12x10^4$ cells/well (AOCS1 $8x10^4$, AOCS7.2 $10x10^4$, AOCS16 $12x10^4$ cells). After 24 hours, each cell line was treated at half the concentration of the respective IC_{50} (determined in the above-described cell viability assay) of either cisplatin (AOCS1: 0.25 µM, AOCS7.2: 0.25 µM; AOCS16: 0.15 µM), paclitaxel (AOCS1: 1.25 nM; AOCS7.2: 50 nM; AOCS16: 0.4 nM) or a combination of both drugs for 24 hours. Cells were rinsed with PBS, trypsinized to form a single-cell suspension and fixed by adding ice-cold 70% ethanol drop-wise. Cells were pelleted and resuspended in a solution containing propidium iodide (0.05 mg/ml) and ribonuclease A (RNase A, Thermo Fisher EN0531, 10 mg/ml). Following 30 to 60 minutes of incubation at

room temperature, DNA content was measured using the FACS Canto LSR II flow cytometer. FlowlogicTM software (Inivai) was used to analyze cell cycle distribution in FL3-A channel applying the Watson pragmatic algorithm (63).

Statistical analyses

Cox proportional hazards models were used to estimate hazard ratios (HRs) with 95% confidence intervals (CIs) using the 'coxph' function of the R package *survival* (v3.2-7). Final models were fitted using Cox regression adjusted for age at diagnosis and FIGO stage. A spline function was used for age at diagnosis with degree of freedom (df) 5 to account for the non-linear effect of the continuous variable. Regression models were fitted separately by histotype. The HGSC regression models were also stratified by site of participant recruitment, and sites with fewer than 10 events within the study period were excluded. The ENOC regression model was not stratified by site due to the limited number of overall patients per site. We also ran sub-analyses adjusting for extent of residual disease and ENOC grade. The OTTA survival dataset was right censored at 10 years from diagnosis to reduce the number of non-ovarian cancer related deaths. In the final Cox regression model, there was evidence for deviation from the proportional hazard assumption, but the degree of deviation was not substantial when considered alongside the large sample size and Schoenfeld residuals. The Kaplan–Meier method was used to estimate and plot progression-free and overall survival probabilities, and the log-rank (Mantel–Cox) test used to compare the survival duration between subgroups. In the Kaplan-Meier curves, the number of patients at risk on the date of diagnosis (time = 0) may be fewer than subsequent time intervals, owing to left truncation of follow-up resulting from delayed study enrolment at some OTTA sites. Differences in proportions of categorical features were assessed by either the chi-square or Fisher's exact test as indicated. Differences in continuous variables were assessed by either a Wilcoxon

Rank Sum Test or a Kruskal-Wallis test. All *in vitro* assays were performed across at least three independent experiments, and data are expressed as mean ± standard error of the mean (SEM) as indicated, from a minimum of three independent measurements. All statistical tests were two-sided and considered significant when $P < 0.05$. Statistical analyses were performed using either GraphPad Prism (v9.3.1) or R (v3.6.3).

Data availability

Genomic variants characterized in the MOCOG study (27), which also includes subjects from the International Cancer Genome Consortium (ICGC) Ovarian Cancer project(3), are available without access restrictions in Synapse under accession code syn34616347 (https://www.synapse.org/#!Synapse:syn34616347). The processed expression and methylation data from the MOCOG study are available without access restrictions in the Gene Expression Omnibus (GEO; https://www.ncbi.nlm.nih.gov/geo/) under accession code GSE211687. Unprocessed methylation data is available from GEO under the accession codes GSE65821 and GSE211687, with no access restrictions. DNA and RNA sequence data generated in the MOCOG and ICGC studies is available from the European Genome-phenome Archive (EGA) repository (https://ega-archive.org) under accession codes EGAS00001005984 and EGAD00001000877, subject to Data Access Committee approvals. Individual participant data from the OTTA study are not publicly available in keeping with the limitations imposed by patient consent and data privacy laws. All other data are provided within the supplementary data files or available upon request to the corresponding author.

Results

Loss of RB1 expression is most frequent in HGSC

RB1 protein expression was assessed by IHC in tumor samples from 7436 patients with ovarian carcinoma using TMAs from 20 centers participating in the OTTA consortium (Table 1, Supplementary Table S1 and Supplementary Table S10). RB1 tumor expression was classified as either retained or lost in 6564 samples, with 872 samples excluded that had either subclonal loss (n = 66), cytoplasmic (n = 17), or uninterpretable results (n = 789) due to either sample drop out or the absence of an internal positive control (Fig. 1A).

RB1 loss was most frequent in HGSC (16.4%), followed by endometrioid ovarian carcinoma (ENOC; 4.1%, Chi-square $P < 0.0001$, Fig. 1B). Loss of RB1 expression was less frequent in all other histotypes (1.8% to 2.8%). *RB1* mRNA expression was also assessed by NanoString in a subset of HGSC tumors (n = 2552) and was significantly associated with RB1 protein expression (Fig. 1C, $P < 0.0001$).

RB1 loss is associated with longer survival in HGSC

Loss of RB1 protein expression was associated with longer OS in patients with HGSC (HR 0.74, 95% CI 0.66-0.83, $P = 6.8 \times 10^{-7}$; Table 2) following multivariate analysis adjusting for stage and age at diagnosis and stratified by study. The effect size was similar after adjustment for the extent of residual disease following cytoreduction (HR 0.66, 95% CI 0.55-0.78, $P = 1.1 \times 10^{-6}$; Supplementary Table S11). Patients with HGSC were comparable in terms of stage regardless of RB1 loss or retained expression (P = 0.9246), however those with RB1 loss had a younger age at diagnosis (median 59 years versus 61 years, P = 0.0003; Supplementary Table S12). Median OS was 4.7 years for patients with RB1 loss compared to 3.6 years for those with retained RB1 expression (Fig. 1D).

In contrast to HGSC, loss of RB1 expression in tumors from patients with ENOC was associated with advanced stage (P = 0.0003), high-grade ($P < 0.0001$) and poorer survival (HR 2.17, 95% CI 1.17-4.03, P = 0.0140; Table 2, Fig. 1E, Supplementary Table S13). RB1

loss and abnormal p53 protein expression, which is highly predictive of *TP53* mutation (64), were strongly correlated (chi-square $P < 0.0001$; Supplementary Fig. S3A). *TP53* mutation is known to be associated with inferior survival in patients with ENOC (38,65), however, we note that combined RB1 loss and abnormal p53 expression were associated with the shortest patient survival (median OS 3.0 years; Supplementary Fig. S3B). While high-grade ENOC showed a higher proportion of RB1 loss (Supplementary Table S13), RB1 loss alone was not significantly associated with survival after adjusting for grade ($P = 0.133$) or the extent of residual disease ($P = 0.107$; Supplementary Table S11 and Supplementary Table S14). Although, the subset of patients with RB1 loss and p53 abnormal ENOC had the poorest survival, regardless of grade (HR 4.91, 95% CI 1.95-12.4, $P < 0.001$) and residual disease (HR 3.78, 95% CI 1.12-12.64, $P = 0.031$; Supplementary Table S11 and Supplementary Table S14).

Combined RB1 loss and germline BRCA*-deficiency *is associated with exceptionally good survival

We previously observed that co-occurrence of somatic RB1 protein loss and *BRCA1* or *BRCA2* alteration (somatic or germline) was associated with longer progression-free survival (PFS) and OS in HGSC (7). Here, germline *BRCA1* and *BRCA2* status was available for 1134 patients with HGSC for which we had RB1 IHC data (Supplementary Fig. S1). Consistent with having a younger age of diagnosis, patients with RB1 loss were more likely to have concurrent g*BRCA*var than those with retained RB1 expression (Fig. 1F, Chi-square $P < 0.0001$; Supplementary Fig. S3C). Patients with both RB1 loss and g*BRCA*var had a 62% reduced risk of death compared to those with g*BRCA*wt and retained RB1 (HR 0.38, 95% CI 0.25-0.58, $P = 5.2 \times 10^{-6}$; Table 2). This association remained significant after adjustment for surgical outcome ($P < 0.001$; Supplementary Table S11). The median OS of g*BRCA*var with

RB1 loss was three times longer than g*BRCA*wt with RB1 retained tumors (median OS 9.3 years vs. 3.1 years, respectively), while median OS was 5.2 years for g*BRCA*var with retained RB1 expression and 4.5 years for g*BRCA*wt with RB1 loss (Fig. 1G; Supplementary Table S15). While there were too few patients to differentiate between *BRCA1* and *BRCA2* variants in the primary regression analysis, a stronger association between RB1 loss and survival was seen in patients with a g*BRCA1*var (median OS 9.3 years RB1 loss vs. 4.7 years RB1 retained) compared to those with a g*BRCA2*var (median OS 8.6 years RB1 loss vs. 5.8 years RB1 retained; Supplementary Fig. S3D, Supplementary Table S16).

Enhanced response to chemotherapy in cells with impaired BRCA and RB1 function

To investigate whether co-occurrence of *RB1* and *BRCA* alterations enhances sensitivity to standard-of-care ovarian cancer drugs, nine patient-derived HGSC cell lines with confirmed pathogenic *TP53* mutation and known *RB1* and *BRCA* status were treated with cisplatin, paclitaxel and olaparib (Supplementary Fig. S4A-B, Supplementary Table S17). AOCS14, the only cell line with a g*BRCA1*var and concomitant loss of RB1 expression, showed the best response to cisplatin and olaparib, and was the second most sensitive cell line to paclitaxel. In contrast AOCS11.2, a line with *BRCA1* promoter methylation and loss of RB1 expression, was relatively resistant to paclitaxel and olaparib. Among cell lines with intact RB1 protein expression and *BRCA* wildtype background, AOCS3 was resistant to cisplatin, paclitaxel and olaparib.

Except for the chemo-naïve cell lines AOCS30 and AOCS14, all other lines were derived from patients previously treated with chemotherapy. Since the evaluation of HGSC cell lines with existing *RB1* alterations may have been confounded by their prior, differential exposure to chemotherapy we therefore characterized responses in isogenically matched lines deleted of *RB1* and/or *BRCA1*. We first inactivated *RB1* in two *BRCA1*-altered (AOCS7.2,

AOCS16) and one wild-type line (AOCS1) using CRISPR-Cas9 (Fig. 2A, Supplementary Fig. S5A). *RB1* knockout clones of the *BRCA1*-altered cell line AOCS7.2 had enhanced sensitivity to cisplatin and paclitaxel compared to *RB1* wild-type clones, which was observed both in short-term drug assays (72 hours, Fig. 2B) and longer-term clonogenic survival assays (12 days, Fig. 2C). In this cell line, sensitivity to cisplatin, paclitaxel and olaparib was increased after *RB1* knockout (cisplatin IC50 1.56 versus 0.38 μM, $P = 0.01$; paclitaxel IC50 92.0 nM versus 11.8 nM, $P = 0.0004$; olaparib IC50 6.1 versus 1.1 nM, $P = 0.0005$; Supplementary Table S18). Further, significantly fewer colonies grew in this *BRCA1*-altered cell line after *RB1* knockout upon treatment with cisplatin ($P = 0.01$), paclitaxel ($P = 0.02$) or a combination of both drugs ($P = 0.067$) in a clonogenic survival assay ($n = 3$). This effect was not apparent in the *BRCA*-wild-type line (AOCS1) or the other *BRCA1*-altered line (AOCS16), except for an increase in sensitivity to olaparib seen in AOCS16 upon RB1 depletion (olaparib IC50 0.072 versus 0.022 nM, $P = 0.04$; Supplementary Table S18). Western blot and IHC analysis (Supplementary Fig. S5A) found that AOCS16 lacked expression of p16, which may functionally disrupt the RB1 pathway irrespective of an *RB1* knockout (66).

Given that RB1 plays a central role in the negative control of the cell cycle (66,67), we tested whether the enhanced chemosensitivity of *RB1* knockout AOCS 7.2 cells was associated with increased cell division. Live cell imaging showed similar growth rates of *RB1* wildtype and knockout clones of all three isogenically matched HGSC cell lines (Supplementary Fig. S5B). In both *BRCA* wild-type and *BRCA1*-altered cell lines, *RB1* knockout did not alter cell cycle distribution at baseline or after 24 hours of cisplatin treatment (Supplementary Fig. S5C). Paclitaxel treatment resulted in a larger proportion of cells with a tetraploid DNA content in *RB1* knockout cells compared to *RB1* wild-type cells, indicating arrest in the G2 or M phase of the cell cycle. This effect was observed in all cell

lines independent of *BRCA* or p16 status, however the arrest was more profound in the AOCS7.2 cell line (AOCS1, G2/M difference 8.59% ± 4.73%, P = 0.144; AOCS16, G2/M difference 8.13% ± 4.45%, P = 0.142; AOCS7.2: G2/M difference 14.49% ± 3.99%, P = 0.022; Supplementary Fig. S5C).

We extended our analysis of isogenically matched pairs by inactivating *BRCA1* and/or *RB1* in the chemo-naïve cell line AOCS30. While we were readily able to establish *RB1* knockout lines, all *BRCA1* targeted clones were hemizygous for *BRCA1* deletion and retained *BRCA1* expression (Supplementary Table S19), suggesting that engineered homozygous loss of *BRCA1* was cell lethal, even in a tumor type where *BRCA1* loss is frequently observed (68).

Genomic and transcriptional landscape of HGSC with combined inactivation of BRCA and RB1

To further understand how RB1 loss may impact the biology of HGSC with co-loss of *BRCA1* or *BRCA2*, we explored matched whole-genome and transcriptome data of primary HGSC tumors in the MOCOG cohort(27) of 126 short- (OS <2 years), moderate- (OS ≥2 to <10 years) and long-term (OS ≥10 years) survivor patients (Supplementary Fig. S1). Each tumor genome was classified according to their HRD and *RB1* status, resulting in 6 groups: *BRCA1*-HRD & *RB1* altered (n = 13); *BRCA1*-HRD & *RB1* wild-type (n = 36); *BRCA2*-HRD & *RB1* altered (n = 8); *BRCA2*-HRD & *RB1* wild-type (n = 20); HRP & *RB1* altered (n = 4), or HRP & *RB1* wild-type (n = 45; Fig. 3A).

The cohort had been selected for a long-term survivor study (27) and hence was enriched for patients with very long survival. Among patients with *BRCA2*-HRD, those with *RB1* alterations had longer OS (median OS 17.0 years) compared with those without *RB1* alterations (median OS 11.7 years, P = 0.0004; Fig. 3B). Similarly, patients with *BRCA1*-

HRD and *RB1* alterations survived longer (median OS 10.4 years) than those with an intact *RB1* gene (median OS 7.1 years). There were few HRP tumors with *RB1* alterations, however these patients had a worse survival (median OS 1.4 years) compared to the HRP group with no *RB1* alteration (median OS 2.4 years).

Examination of genomic features revealed relatively similar patterns within *BRCA1*-HRD and *BRCA2*-HRD groups, although there were a few discriminatory features identified between those with and without *RB1* alterations (Supplementary Fig. S6 and Supplementary Fig. S7, Supplementary Table S2). For example, the *BRCA1*-associated rearrangement signature Ovary_G (69) was more enriched in *BRCA1*-HRD tumors with *RB1* alterations compared to those without (P = 0.039). Among *BRCA2*-HRD tumors, the mutational signatures DBS6 (unknown etiology) and SBS3 (associated with HRD) (70) were higher in *RB1*-altered tumors compared to non-altered tumors, although this was not significant (P = 0.082 and P = 0.1 respectively). Concordantly, the average *BRCA1*-type and *BRCA2*-type CHORD scores (41) were highest in *BRCA1*- and *BRCA2*-HRD tumors with *RB1* alterations respectively, indicating a higher probability of HRD. As described previously (71), *CCNE1* gene amplifications were absent in tumors with both HRD and *RB1* alterations (P = 0.0006; Supplementary Fig. S8).

We hypothesized that tumors with combined HRD and *RB1* loss may have unique transcriptional profiles. To explore this, we compared gene expression profiles between each HRD/*RB1* group and the reference set of tumors that were HRP and *RB1* wild-type (Supplementary Table S4, Supplementary Fig. S9). There was significant enrichment of MSigDB hallmark gene sets among genes differentially expressed in *BRCA1*-HRD tumors with *RB1* alterations, the most prominent being interferon gamma response (up), interferon alpha response (up), oxidative phosphorylation (up), and E2F targets (up; adjusted P < 0.0001; Fig. 4A). The differentially expressed genes identified between *BRCA2*-HRD / *RB1*

altered tumors and the reference set were significantly enriched for the MSigDB hallmark gene sets: E2F targets (up), epithelial mesenchymal transition (down), G2M checkpoint (up), and TNF alpha signaling via NF-kB (up; adjusted $P < 0.0001$).

Inference of immune cell subsets (72) showed enrichment of follicular helper T cells in *BRCA2*-HRD / *RB1* altered tumors (adjusted $P = 0.094$), and regulatory T cells in *BRCA1*-HRD / *RB1* altered tumors (adjusted $P = 0.016$), compared to HRP / *RB1* wild-type tumors (Supplementary Fig. S10, Supplementary Table S20). Upregulation of immune-related transcription was particularly apparent in the *BRCA1*-HRD / *RB1* altered tumors, which were the only subgroup to show increased cGAS-STING ($P = 0.0024$) and toll-like receptor signaling pathway activity ($P = 0.04$; Fig. 4B). Concordantly, *BRCA1*-HRD / *RB1* altered tumors displayed evidence of increased expression of MHC Class I molecules (Fig. 4C).

Since enhanced tumor cell proliferation has been associated with long-term survival in HGSC (7,27), and loss of RB1 might accelerate proliferation (32), we evaluated the expression of proliferation markers across the *RB1* and *BRCA* subgroups. *BRCA1*-HRD tumors with *RB1* alterations had significantly higher mRNA levels of the cell proliferation related genes *PCNA* (proliferating cell nuclear antigen) and *MCM3* (minichromosome maintenance complex component 3) compared to *BRCA1*-HRD tumors without *RB1* alterations ($P < 0.0001$, Supplementary Fig. S7). However, there were no significant differences in the proportion of Ki-67 positive cancer cell nuclei ($P = 0.3297$) across the subgroups (Supplementary Fig. S7), which was previously quantified by immunohistochemistry (7) in a subset of primary tumors ($n = 59$).

Patients with germline BRCA deficiency and somatic loss of RB1 tumor expression show elevated immune activity

Having observed that HGSC with combined RB1 loss and HRD have enrichment of transcriptional signatures associated with an enhanced immune response, we accessed existing immunohistochemical data (40) to determine the prevalence of CD8+ TILs in HGSC samples that also had RB1 protein expression and *BRCA* germline status (n = 868). Patients with g*BRCA*var and RB1 loss had a significantly higher proportion of tumors (79.6%) with moderate and high densities of CD8+ TILs, compared to g*BRCA*var with retained RB1 (64.9%), g*BRCA*wt with RB1 loss (72.4%) and g*BRCA*wt with retained RB1 (63.6%, P = 0.0264; Fig. 4D). Tumors with complete absence of CD8+ TILs were the least frequent in g*BRCA*var with RB1 loss (4.1%) compared to the other groups (13.8% of g*BRCA*var with retained RB1 tumor expression, 14.6% of g*BRCA*wt with RB1 tumor loss, 18.8% of g*BRCA*wt with retained RB1 tumor expression).

Gene expression-based molecular subtypes (13,39) also differed by RB1 and *BRCA* status (P = 0.0271, n = 601; Fig. 4E). As expected, there was enrichment for the C2/immunoreactive subtype, a subtype characterized by the presence of intratumoral CD8+ T cells and good survival, in g*BRCA*var with RB1 loss (32.4%) compared to the other subgroups (between 19.8% and 23.4%). Additionally, tumors with RB1 loss were enriched for the C4/differentiated molecular subtype, a subtype characterized by cytokine expression and good survival, regardless of *BRCA* status (45.9% in g*BRCA*var with RB1 loss, 50.0% in g*BRCA*wt with RB1 loss, 39.5% in g*BRCA*var with retained RB1, 32.1% of g*BRCA*wt with retained RB1). g*BRCA*var with RB1 loss also had the lowest proportion of the C5/proliferative molecular subtype (2.7% versus 17.2% to 20.3% in the other groups), a subtype associated with diminished immune cell infiltration and poor survival (13,20).

Discussion

Identifying the determinants of long-term patient survival, particularly in cancers with a generally unfavorable prognosis such as HGSC, may reveal novel therapeutic targets and inform personalized treatment strategies (8). Improved survival associated with RB1 loss has been described previously in HGSC (35,36,73), including in the context of co-occurring HR gene alterations (7,74), but the underlying factors contributing to this survival benefit have not been studied to date. We assessed tumor samples from a cohort of more than 7,000 patients with ovarian carcinoma, including a subset with high resolution genomic data, to understand how RB1 loss may impact on therapeutic response and patient survival.

Alteration of the RB1 pathway is a frequent event in tumorigenesis, including loss of regulators such as p16, activation of D- and E-type cyclins and their associated cyclin dependent kinases, and loss of RB1 itself (reviewed in (75)). Our study showed that RB1 loss is associated with longer survival in patients with advanced stage HGSC, but by contrast, loss of RB1 in ENOC was associated with a shorter survival, particularly in combination with p53 mutation, suggesting that loss of RB1 and *TP53* mutation have a compounding negative impact on survival in patients with ENOC. This casts doubt on the rationale of grouping p53 abnormal ENOC with HGSC in clinical trials. Despite suggestions from its endometrial counterpart (76), we are not aware of large studies confirming HRD in high-grade or p53 abnormal ENOC and the only rationale to combine them with HGSC may be a historical problem in the pathological classification of these tumors (77). Similar to ENOC, in prostate cancer, RB1 loss is associated with poorer survival: early somatic co-deletion of *BRCA2* and *RB1* is associated with an aggressive, castration-resistant prostate cancer subtype (CRPC) characterized by epithelial-to-mesenchymal transition and shorter survival (30). RB1 loss appears to facilitate lineage plasticity and, with p53-comutation, leads to an androgen-independent prostate cancer phenotype (78,79) and consequently resistance to anti-androgen therapy.

Triple negative breast cancer (TNBC) provides an important paralell to the findings for RB1 loss in HGSC. In TNBC, RB1 loss is most common in the basal-like subtype, where *BRCA1* inactivation is associated with frequent *RB1* gene disruption and RB1 loss (29). RB1 loss alone, as well as co-occurrence with *BRCA1* promoter hypermethylation, is associated with a favorable chemotherapy response and outcome (28,80-82). Notably, TNBC and HGSC are more similar than the cancers that they are grouped with anatomically, sharing gene expression patterns, genetic drivers including *BRCA1* and *BRCA2*, ubiquitous loss of *TP53*, extensive copy number variation, and susceptibility to platinum-based chemotherapy (83,84). Taken together, the relationship between RB1 loss and patient survival appears to be dependent on the histotype and/or the molecular context (85).

Some, but not all TNBC and early metastatic prostate cancers are associated with germline variants in *BRCA1*, *BRCA2* and other genes involved in HR DNA repair. However, previous tumor studies of RB1 expression have not also defined the HRD status of individual samples. A strength of this study was the known *BRCA* germline status of 1134 of the patients with HGSC for which we also had RB1 protein expression, and this revealed the strong association of co-alteration in either *BRCA1* or *BRCA2* and *RB1* with survival, regardless of the extent of residual disease following primary debulking surgery. In addition to germline pathogenic variants in *BRCA1* or *BRCA2*, germline or somatic inactivation of other genes involved in HR DNA repair, such as *RAD51C*, can result in a similar molecular phenotype, characterized by distinct genomic scarring (27). Using whole-genome sequence data, we determined the likely tumor HRD status in a subset of 126 tumors using an algorithm that recognizes genomic scarring associated with HRD (Fig. 3A), rather than simply designating *BRCA* alteration status, which does not account for all mechanisms of HR repair inactivation (86). Although the number of samples with RB1 loss and HR proficiency was small, the very poor outcome we observed within this group suggests that RB1 loss may

only be associated with better survival in an HRD background. Validation of this finding in a larger cohort may further inform how RB1 loss could favorably influence survival in certain histological and molecular contexts.

We have previously noted that enhanced proliferation in HGSC is associated with long-term survival (7,27) and it is reasonable to suggest that RB1 loss may be imparting an effect through deregulating the cell cycle. However, data on the effect of RB1 loss on proliferation in HGSC tumors and cancer cell lines is inconsistent. *RB1* knockout in our HGSC cell lines did not cause cell cycle alterations in the absence of treatment, and despite differences in proliferative markers at the mRNA level, there was no significant difference in the proportion of Ki-67 positive nuclei between tumors with or without RB1 protein expression. In a recent OTTA study, Ki-67 expression was not associated with survival in HGSC; however, there was strong correlation between loss of RB1 and the proliferative marker MCM3 (87), which may provide a more accurate measure of tumor cell proliferation than Ki-67 (88).

In addition to its role in driving progression through the G1 stage of the cell cycle, RB1 has non-canonical functions. RB1 has been shown to participate in HR DNA repair through interactions with BRG1 and ATM (89). A recent pan-cancer study (90) found that combined loss of *TP53* and *RB1* was associated with a particularly high genome-wide loss-of-heterozygosity score, one of the key elements of genomic scarring associated with HRD. In our whole-genome analysis, HGSC tumors with dual loss of HRD and *RB1* did not exhibit overall higher mutation burden; however, we did observe elevated levels of mutational signatures associated with HRD, which may be evidence of compounding DNA repair defects. It remains possible that the combined inactivation of RB1 and HR genes contribute to enhanced chemotherapy response and/or an impaired ability for tumor cells to develop therapy resistance.

When we evaluated a set of patient-derived HGSC lines, those with *BRCA1* and *RB1* alterations were most sensitive to cisplatin and olaparib. Knockout of *RB1* in the AOCS 7.2 cell line which had a pre-existing *BRCA1* alteration, resulted in an increase in chemosensitivity, consistent with the notion that co-loss enhances chemotherapy response (7). Unfortunately, despite considerable efforts, we were unable to generate a larger series of isogenically matched cell lines with combinations of conditional knockouts of *RB1* and *BRCA1* as all surviving clones retained at least one *BRCA1* allele. *BRCA1* loss is embryonic lethal and engineered loss in cell lines has been reported as lethal elsewhere including in the human haploid cell line, HAP1 (68).

The survival benefit associated with RB1 loss was more pronounced in patients with germline *BRCA1* variants compared to those with germline *BRCA2* variants. This is somewhat unexpected, given the increasing evidence that *BRCA2* loss appears to confer a greater survival advantage than *BRCA1* loss, especially at 10 years since diagnosis (24,27). These differences could be partially explained by the increased immune activity observed in tumors with RB1 loss, particularly prevalent in *BRCA1*-HRD / RB1-altered HGSC. This group showed the strongest cGAS-STING pathway activity, suggesting that RB1 loss may further enhance cytosolic DNA-dependent type I interferon (IFN) signaling, which is thought to be associated with *BRCA1* loss in HGSC (91). RB1 has been shown to inhibit innate IFN-β production in immunocompetent mice (92) and RB1 deficiency triggered an increased IFN-β and IFN-α secretion. Co-mutation of *RB1* and *TP53* was recently found to be associated with an enhanced response to the immune checkpoint inhibitor atezolizumab in metastatic urothelial bladder cancer (93). Similarly, a case report described a complete response to atezolizumab in heavily pre-treated, RB1-negative TNBC (94). This generates the hypothesis that RB1 loss could predict response to such therapies in HGSC, since this tumor type ubiquitously harbors *TP53* mutations (95). However, a recent biomarker study in patients

with ovarian cancer treated with atezolizumab or placebo and standard chemotherapy found that deleterious mutations in *RB1* were prognostic for a better PFS, regardless of the addition of atezolizumab (96). While it appears RB1 loss alone may not be predictive of response to the PD-L1 inhibitor atezolizumab, response rates to PD-1/PD-L1 pathway checkpoint inhibitors are generally quite low in HGSC, with the best objective response rates between 8% and 15% (97). Our study has identified a subset of patients with combined RB1 and *BRCA* inactivation who demonstrate exceptional immune responses and may provide clues for the development of new immunotherapeutic strategies for HGSC that extend beyond targeting PD-L1/PD-1.

Our work highlights the importance of RB1 loss to treatment response and survival and focuses attention on other therapeutic opportunities in this subset of HGSC. Approximately 20 percent of HGSC have somatic loss of *RB1* assessed using genomic data (3,27), a figure that is consistent with the immunohistochemical results obtained in the large patient cohort described here. Both approaches indicate that RB1 loss is generally clonal, enhancing its value as a therapeutic target if selective inhibitors can be identified. While subclonal RB1 loss appears to be rare in ovarian carcinoma (0.89%), the relevance of subclonal RB1 loss should be studied in the future using full-faced tumor sections, and ideally paired primary and relapse specimens to assess clonality over time. Casein kinase 2 (CK2) inhibitors have been reported to enhance the sensitivity of *RB1*-deficient TNBC and HGSC cells to carboplatin and niraparib (bioRxiv https://doi.org/10.1101/2022.11.14.516369). In addition, Aurora kinase A and B inhibition is synthetically lethal in combination with RB1 loss in breast and lung cancer cells (98-100). Irrespective of HRD status, *RB1* mutations correlate with sensitivity to WEE1 inhibition in *TP53* mutant TNBC and patient-derived HGSC xenografts (101), indicating additional treatment options that exploit RB1 inactivation in these tumors. In this study, the *BRCA1*-

altered cell line AOCS7.2 with induced *RB1* knockout was more sensitive to olaparib suggesting that RB1 loss may also predict responses to PARP inhibitors in HGSC. Most participants in the current study were diagnosed before PARP inhibitor use and *BRCA* testing was common (95% enrolled before 2013), however our findings provide a genuine hypothesis that patients with RB1 loss may derive greater benefit from PARP inhibitors, which could be tested in newer cohorts. RB1 staining of tumor tissue by IHC is a relatively low-cost pathology-based assay that could be used in prospective studies to test whether RB1 expression is predictive of responses to PARP inhibitors, either alone or in combination with approved HRD tests.

Authors' Contributions

MK, SJR, DDLB and DWG conceived the study design. FAMS, KT, KP, JB and TH carried out experiments, and analyzed and interpreted results along with TB, AP, DA, TZ, NSM, SF, AD, MK, SJR, DDLB and DWG. MK assessed and interpreted immunohistochemical scores. All authors contributed through recruitment and consenting of patients, collection and processing of biological samples, clinical care, abstraction and curation of clinical data and maintenance of follow-up. DDLB and DWG supervised the study and together with FAMS and KT wrote the manuscript. All authors contributed to writing, review and revision of the manuscript and approved the final submitted version.

Acknowledgments

We thank J. Beach and L. Bowes for their contributions to the study. This work was supported by the National Health and Medical Research Council (NHMRC) of Australia (1186505 to DWG; 1092856, 1117044 and 2008781 to DDLB; 2009840 to SJR), the National Institutes of Health (NIH) / National Cancer Institute (R01CA172404 to SJR, P50

CA136393 to SHK) and the U.S. Army Medical Research and Materiel Command Ovarian Cancer Research Program (Award No. W81XWH-16-2-0010 and W81XWH-21-1-0401). DWG is supported by a Victorian Cancer Agency / Ovarian Cancer Australia Low-Survival Cancer Philanthropic Mid-Career Research Fellowship (MCRF22018). FAMS is supported by a Swiss National Foundation Early Postdoc Mobility Fellowship (P2BEP3-172246), a Swiss Cancer League grant BIL KFS-3942-08-2016, the Foundation for Clinical-Experimental Cancer Research (Bern, Switzerland), and a Prof. Max Cloëtta foundation grant. KIP is supported by a NHMRC CJ Martin Overseas Biomedical Fellowship (APP1111032). ELC is supported by a Victorian Cancer Agency Mid-Career Fellowship (MCRF21004). MW is supported by the European Research Council under the European Union's Horizon 2020 Research and Innovation Programme grant agreement No 742432 (BRCA-ERC). KS is supported by the Swedish Cancer Foundation. MSA is funded through a Michael Smith Health Research BC Scholar Award (18274) and the Janet D. Cottrelle Foundation Scholars program managed by the BC Cancer Foundation.

BC's Gynecological Cancer Research team (OVCARE) receives support through the BC Cancer Foundation and the VGH & UBC Hospitals Foundation. The Gynaecological Oncology Biobank at Westmead was funded by the NHMRC (ID310670, ID628903); the Cancer Institute NSW (12/RIG/1-17, 15/RIG/1-16); and acknowledges support from the Department of Gynaecological Oncology, Westmead Hospital, and the Sydney West Translational Cancer Research Centre (Cancer Institute NSW 15/TRC/1-01). The Women's Cancer Research Program at Cedars-Sinai Medical Center (LAX) is supported by The National Center for Advancing Translational Sciences (NCATS) Grant UL1TR000124. The Study of Epidemiology and Risk Factors in Cancer Heredity (SEARCH) is funded by Cancer Research UK (C490/A10119 C490/A10124 C490/A16561) and the UK National Institute for Health Research Biomedical Research Centre at the University of Cambridge. The UKOPS

study was funded by The Eve Appeal (The Oak Foundation) with contribution to authors' salary through MRC core funding MC_UU_00004/01 and the National Institute for Health Research University College London Hospitals Biomedical Research Centre.

The investigators also acknowledge generous contributions from the Border Ovarian Cancer Awareness Group, the Peter MacCallum Cancer Foundation, the Graf Family Foundation, Wendy Taylor, Arthur Coombs and family, and the Piers K Fowler Fund. The contents of the published material are solely the responsibility of the authors and do not reflect the views of the NHMRC, NIH, and other funders.

This article is dedicated to the memory of Prof. Naveena Singh. An anatomical pathologist specializing in gynecological cancer research, Prof. Singh made a significant contribution to the assessment and classification of tumor tissue samples in this study. She passed away in 2023.

REFERENCES

1. Bowtell DD, Böhm S, Ahmed AA, Aspuria P-J, Bast RC, Beral V*, et al.* Rethinking ovarian cancer II: reducing mortality from high-grade serous ovarian cancer. *Nature Reviews Cancer* 2015;**15**(11):668-79 doi 10.1038/nrc4019.
2. Norquist B, Wurz KA, Pennil CC, Garcia R, Gross J, Sakai W*, et al.* Secondary somatic mutations restoring BRCA1/2 predict chemotherapy resistance in hereditary ovarian carcinomas. *Journal of Clinical Oncology* 2011;**29**(22):3008-15 doi 10.1200/JCO.2010.34.2980.
3. Patch AM, Christie EL, Etemadmoghadam D, Garsed DW, George J, Fereday S*, et al.* Whole-genome characterization of chemoresistant ovarian cancer. *Nature* 2015;**521**(7553):489-94 doi 10.1038/nature14410.

4. Burdett NL, Willis MO, Alsop K, Hunt AL, Pandey A, Hamilton PT*, et al.* Multiomic analysis of homologous recombination-deficient end-stage high-grade serous ovarian cancer. *Nature Genetics* 2023;**55**(3):437-50 doi 10.1038/s41588-023-01320-2.

5. Gockley A, Melamed A, Bregar AJ, Clemmer JT, Birrer M, Schorge JO*, et al.* Outcomes of Women With High-Grade and Low-Grade Advanced-Stage Serous Epithelial Ovarian Cancer. *Obstetrics and Gynecology* 2017;**129**(3):439-47 doi 10.1097/AOG.0000000000001867.

6. Dao F, Schlappe BA, Tseng J, Lester J, Nick AM, Lutgendorf SK*, et al.* Characteristics of 10-year survivors of high-grade serous ovarian carcinoma. *Gynecologic Oncology* 2016;**141**(2):260-3 doi 10.1016/j.ygyno.2016.03.010.

7. Garsed DW, Alsop K, Fereday S, Emmanuel C, Kennedy CJ, Etemadmoghadam D*, et al.* Homologous recombination DNA repair pathway disruption and retinoblastoma protein loss are associated with exceptional survival in high-grade serous ovarian cancer. *Clinical Cancer Research* 2018;**24**(3):569-80 doi 10.1158/1078-0432.CCR-17-1621.

8. Saner FAM, Herschtal A, Nelson BH, DeFazio A, Goode EL, Ramus SJ*, et al.* Going to extremes: determinants of extraordinary response and survival in patients with cancer. *Nature Reviews Cancer* 2019;**19**(6):339-48 doi 10.1038/s41568-019-0145-5.

9. Takenaka M, Köbel M, Garsed DW, Fereday S, Pandey A, Etemadmoghadam D*, et al.* Survival following chemotherapy in ovarian clear cell carcinoma is not associated with pathological misclassification of tumor histotype. *Clinical Cancer Research* 2019;**25**(13):3962-73 doi 10.1158/1078-0432.CCR-18-3691.

10. du Bois A, Reuss A, Pujade-Lauraine E, Harter P, Ray-Coquard I, Pfisterer J. Role of surgical outcome as prognostic factor in advanced epithelial ovarian cancer: A combined exploratory analysis of 3 prospectively randomized phase 3 multicenter trials. *Cancer* 2009;**115**(6):1234-44 doi 10.1002/cncr.24149.

11. Wallace S, Kumar A, Mc Gree M, Weaver A, Mariani A, Langstraat C*, et al.* Efforts at maximal cytoreduction improve survival in ovarian cancer patients, even when complete gross resection is not feasible. *Gynecologic Oncology* 2017;**145**(1):21-6 doi 10.1016/j.ygyno.2017.01.029.

12. Harter P, Sehouli J, Vergote I, Ferron G, Reuss A, Meier W*, et al.* Randomized Trial of Cytoreductive Surgery for Relapsed Ovarian Cancer. *New England Journal of Medicine* 2021;**385**(23):2123-31 doi 10.1056/NEJMoa2103294.

13. Tothill RW, Tinker AV, George J, Brown R, Fox SB, Lade S*, et al.* Novel molecular subtypes of serous and endometrioid ovarian cancer linked to clinical outcome. *Clinical Cancer Research* 2008;**14**(16):5198-208 doi 10.1158/1078-0432.CCR-08-0196.

14. Liu Z, Beach JA, Agadjanian H, Jia D, Aspuria PJ, Karlan BY*, et al.* Suboptimal cytoreduction in ovarian carcinoma is associated with molecular pathways characteristic of increased stromal activation. *Gynecologic Oncology* 2015;**139**(3):394-400 doi 10.1016/j.ygyno.2015.08.026.

15. Wang C, Armasu SM, Kalli KR, Maurer MJ, Heinzen EP, Keeney GL*, et al.* Pooled Clustering of High-Grade Serous Ovarian Cancer Gene Expression Leads to Novel Consensus Subtypes Associated with Survival and Surgical Outcomes. *Clinical Cancer Research* 2017;**23**(15):4077-85 doi 10.1158/1078-0432.CCR-17-0246.

16. Torres D, Kumar A, Bakkum-Gamez JN, Weaver AL, McGree ME, Wang C*, et al.* Mesenchymal molecular subtype is an independent predictor of severe postoperative complications after primary debulking surgery for advanced ovarian cancer. *Gynecologic Oncology* 2019;**152**(2):223-7 doi 10.1016/j.ygyno.2018.11.019.

17. Zhang L, Conejo-Garcia JR, Katsaros D, Gimotty PA, Massobrio M, Regnani G*, et al.* Intratumoral T Cells, Recurrence, and Survival in Epithelial Ovarian Cancer. *New England Journal of Medicine* 2003;**348**(3):203-13 doi 10.1056/nejmoa020177.

18. Hwang WT, Adams SF, Tahirovic E, Hagemann IS, Coukos G. Prognostic significance of tumor-infiltrating T cells in ovarian cancer: A meta-analysis. *Gynecologic Oncology* 2012;**124**(2):192-8 doi 10.1016/j.ygyno.2011.09.039.

19. Fong PC, Yap TA, Boss DS, Carden CP, Mergui-Roelvink M, Gourley C*, et al.* Poly(ADP)-ribose polymerase inhibition: frequent durable responses in BRCA carrier ovarian cancer correlating with platinum-free interval. *Journal of Clinical Oncology* 2010;**28**(15):2512-9 doi 10.1200/JCO.2009.26.9589.

20. The Cancer Genome Atlas Research Network. Integrated genomic analyses of ovarian carcinoma. *Nature* 2011;**474**(7353):609-15 doi 10.1038/nature10166.

21. Pennington KP, Walsh T, Harrell MI, Lee MK, Pennil CC, Rendi MH*, et al.* Germline and somatic mutations in homologous recombination genes predict platinum response and survival in ovarian, fallopian tube, and peritoneal carcinomas. *Clinical Cancer Research* 2014;**20**(3):764-75 doi 10.1158/1078-0432.CCR-13-2287.

22. Bolton KL, Chenevix-Trench G, Goh C, Sadetzki S, Ramus SJ, Karlan BY*, et al.* Association between BRCA1 and BRCA2 mutations and survival in women with invasive epithelial ovarian cancer. *JAMA* 2012;**307**(4):382-90 doi 10.1001/jama.2012.20.

23. Alsop K, Fereday S, Meldrum C, DeFazio A, Emmanuel C, George J*, et al.* BRCA mutation frequency and patterns of treatment response in BRCA mutation-positive women with ovarian cancer: A report from the Australian ovarian cancer study group. *Journal of Clinical Oncology* 2012;**30**(21):2654-63 doi 10.1200/JCO.2011.39.8545.

24. Candido-dos-Reis FJ, Song H, Goode EL, Cunningham JM, Fridley BL, Larson MC*, et al.* Germline mutation in BRCA1 or BRCA2 and ten-year survival for women diagnosed with epithelial ovarian cancer. *Clinical Cancer Research* 2015;**21**(3):652-7 doi 10.1158/1078-0432.CCR-14-2497.

25. Wang Y, Bernhardy AJ, Cruz C, Krais JJ, Nacson J, Nicolas E*, et al.* The BRCA1-Δ11q alternative splice isoform bypasses germline mutations and promotes therapeutic resistance to PARP inhibition and cisplatin. *Cancer Research* 2016;**76**(9):2778-90 doi 10.1158/0008-5472.CAN-16-0186.

26. Maxwell KN, Wubbenhorst B, Wenz BM, De Sloover D, Pluta J, Emery L*, et al.* BRCA locus-specific loss of heterozygosity in germline BRCA1 and BRCA2 carriers. *Nature Communications* 2017;**8**(1):319- doi 10.1038/s41467-017-00388-9.

27. Garsed DW, Pandey A, Fereday S, Kennedy CJ, Takahashi K, Alsop K*, et al.* The genomic and immune landscape of long-term survivors of high-grade serous ovarian cancer. *Nature Genetics* 2022;**54**(12):1853-64 doi 10.1038/s41588-022-01230-9.

28. Stefansson OA, Jonasson JG, Olafsdottir K, Hilmarsdottir H, Olafsdottir G, Esteller M*, et al.* CpG island hypermethylation of BRCA1 and loss of pRb as co-occurring events in basal/triple-negative breast cancer. *Epigenetics* 2011;**6**(5):638-49 doi 10.4161/epi.6.5.15667.

1060 29. Jönsson G, Staaf J, Vallon-Christersson J, Ringnér M, Gruvberger-Saal SK, Saal LH*, et*
1061 *al.* The Retinoblastoma Gene Undergoes Rearrangements in BRCA1 -Deficient Basal-
1062 like Breast Cancer. *Cancer Research* 2012;**72**(16):4028-36 doi 10.1158/0008-
1063 5472.CAN-12-0097.
1064 30. Chakraborty G, Armenia J, Mazzu YZ, Nandakumar S, Stopsack KH, Atiq MO*, et al.*
1065 Significance of BRCA2 and RB1 co-loss in aggressive prostate cancer progression.
1066 *Clinical Cancer Research* 2020;**26**(8):2047-64 doi 10.1158/1078-0432.CCR-19-1570.
1067 31. Chen WS, Alshalalfa M, Zhao SG, Liu Y, Mahal BA, Quigley DA*, et al.* Novel RB1-Loss
1068 Transcriptomic Signature Is Associated with Poor Clinical Outcomes across Cancer
1069 Types. *Clinical Cancer Research* 2019;**25**(14):4290-9 doi 10.1158/1078-0432.CCR-19-
1070 0404.
1071 32. Burkhart DL, Sage J. Cellular mechanisms of tumour suppression by the
1072 retinoblastoma gene. *Nature Reviews Cancer* 2008;**8**(9):671-82 doi 10.1038/nrc2399.
1073 33. Knudsen ES, Knudsen KE. Tailoring to RB: tumour suppressor status and therapeutic
1074 response. *Nature Reviews Cancer* 2008;**8**(9):714-24 doi 10.1038/nrc2401.
1075 34. Vélez-Cruz R, Manickavinayaham S, Biswas AK, Clary RW, Premkumar T, Cole F*, et al.*
1076 RB localizes to DNA double-strand breaks and promotes DNA end resection and
1077 homologous recombination through the recruitment of BRG1. *Genes and*
1078 *Development* 2016;**30**(22):2500-12 doi 10.1101/gad.288282.116.
1079 35. Millstein J, Budden T, Goode EL, Anglesio MS, Talhouk A, Intermaggio MP*, et al.*
1080 Prognostic gene expression signature for high-grade serous ovarian cancer. *Annals of*
1081 *Oncology* 2020;**31**(9):1240-50 doi 10.1016/j.annonc.2020.05.019.
1082 36. Milea A, George SHL, Matevski D, Jiang H, Madunic M, Berman HK*, et al.*
1083 Retinoblastoma pathway deregulatory mechanisms determine clinical outcome in

high-grade serous ovarian carcinoma. *Modern Pathology* 2014;**27**(7):991-1001 doi 10.1038/modpathol.2013.218.

37. Sieh W, Köbel M, Longacre TA, Bowtell DD, deFazio A, Goodman MT*, et al.* Hormone-receptor expression and ovarian cancer survival: An Ovarian Tumor Tissue Analysis consortium study. *The Lancet Oncology* 2013;**14**(9):853-62 doi 10.1016/S1470-2045(13)70253-5.

38. Köbel M, Kang EY, Weir A, Rambau PF, Lee CH, Nelson GS*, et al.* p53 and ovarian carcinoma survival: an Ovarian Tumor Tissue Analysis consortium study. *The Journal of Pathology: Clinical Research* 2023;**9**(3):208-22 doi 10.1002/cjp2.311.

39. Talhouk A, George J, Wang C, Budden T, Tan TZ, Chiu DS*, et al.* Development and Validation of the Gene Expression Predictor of High-grade Serous Ovarian Carcinoma Molecular SubTYPE (PrOTYPE). *Clinical Cancer Research* 2020;**26**(20):5411-23 doi 10.1158/1078-0432.CCR-20-0103.

40. Ovarian Tumor Tissue Analysis (OTTA) Consortium, Goode EL, Block MS, Kalli KR, Vierkant RA, Chen W*, et al.* Dose-Response Association of CD8+ Tumor-Infiltrating Lymphocytes and Survival Time in High-Grade Serous Ovarian Cancer. *JAMA Oncology* 2017;**3**(12):e173290-e doi 10.1001/jamaoncol.2017.3290.

41. Nguyen L, W. M. Martens J, Van Hoeck A, Cuppen E. Pan-cancer landscape of homologous recombination deficiency. *Nature Communications* 2020;**11**(1):1-12 doi 10.1038/s41467-020-19406-4.

42. Love MI, Huber W, Anders S. Moderated estimation of fold change and dispersion for RNA-seq data with DESeq2. *Genome Biology* 2014;**15**(12):550- doi 10.1186/s13059-014-0550-8.

1107 43. Horton R, Wilming L, Rand V, Lovering RC, Bruford EA, Khodiyar VK*, et al.* Gene map
1108 of the extended human MHC. *Nature Reviews Genetics* 2004;**5**(12):889-99 doi
1109 10.1038/nrg1489.
1110 44. Liberzon A, Birger C, Thorvaldsdóttir H, Ghandi M, Mesirov JP, Tamayo P. The
1111 Molecular Signatures Database Hallmark Gene Set Collection. *Cell Systems*
1112 2015;**1**(6):417-25 doi 10.1016/j.cels.2015.12.004.
1113 45. Belinky F, Nativ N, Stelzer G, Zimmerman S, Iny Stein T, Safran M*, et al.* PathCards:
1114 multi-source consolidation of human biological pathways. *Database* 2015;**2015**(2):1-
1115 13 doi 10.1093/database/bav006.
1116 46. Christie EL, Pattnaik S, Beach J, Copeland A, Rashoo N, Fereday S*, et al.* Multiple
1117 ABCB1 transcriptional fusions in drug resistant high-grade serous ovarian and breast
1118 cancer. *Nature Communications* 2019;**10**(1):1295- doi 10.1038/s41467-019-09312-9.
1119 47. Domcke S, Sinha R, Levine DA, Sander C, Schultz N. Evaluating cell lines as tumour
1120 models by comparison of genomic profiles. *Nature Communications* 2013;**4**(2126)
1121 doi 10.1038/ncomms3126.
1122 48. Barretina J, Caponigro G, Stransky N, Venkatesan K, Margolin AA, Kim S*, et al.* The
1123 Cancer Cell Line Encyclopedia enables predictive modelling of anticancer drug
1124 sensitivity. *Nature* 2012;**483**(7391):603-7 doi 10.1038/nature11003.
1125 49. Cerami E, Gao J, Dogrusoz U, Gross BE, Sumer SO, Aksoy BA*, et al.* The cBio Cancer
1126 Genomics Portal: An open platform for exploring multidimensional cancer genomics
1127 data. *Cancer Discovery* 2012;**2**(5):401-4 doi 10.1158/2159-8290.CD-12-0095.
1128 50. Delahunty R, Nguyen L, Craig S, Creighton B, Ariyaratne D, Garsed DW*, et al.*
1129 TRACEBACK: Testing of Historical Tubo-Ovarian Cancer Patients for Hereditary Risk

Genes as a Cancer Prevention Strategy in Family Members. *Journal of Clinical Oncology* 2022;**40**(18):2036-47 doi 10.1200/JCO.21.02108.

51. Gao J, Aksoy BA, Dogrusoz U, Dresdner G, Gross B, Sumer SO*, et al.* Integrative analysis of complex cancer genomics and clinical profiles using the cBioPortal. *Science Signaling* 2013;**6**(269):1-20 doi 10.1126/scisignal.2004088.

52. Ghandi M, Huang FW, Jané-Valbuena J, Kryukov GV, Lo CC, McDonald ER*, et al.* Next-generation characterization of the Cancer Cell Line Encyclopedia. *Nature* 2019;**569**(7757):503-8 doi 10.1038/s41586-019-1186-3.

53. Landrum MJ, Lee JM, Benson M, Brown GR, Chao C, Chitipiralla S*, et al.* ClinVar: improving access to variant interpretations and supporting evidence. *Nucleic Acids Research* 2018;**46**(D1):D1062-D7 doi 10.1093/nar/gkx1153.

54. Etemadmoghadam D, Defazio A, Beroukhim R, Mermel C, George J, Getz G*, et al.* Integrated genome-wide DNA copy number and expression analysis identifies distinct mechanisms of primary chemoresistance in ovarian carcinomas. *Clinical Cancer Research* 2009;**15**(4):1417-27 doi 10.1158/1078-0432.CCR-08-1564.

55. Ran FA, Hsu PD, Wright J, Agarwala V, Scott DA, Zhang F. Genome engineering using the CRISPR-Cas9 system. *Nature Protocols* 2013;**8**(11):2281-308 doi 10.1038/nprot.2013.143.

56. Lawhorn IEB, Ferreira JP, Wang CL. Evaluation of sgRNA target sites for CRISPR-mediated repression of TP53. *PloS one* 2014;**9**(11):e113232-e doi 10.1371/journal.pone.0113232.

57. Liang X, Potter J, Kumar S, Zou Y, Quintanilla R, Sridharan M*, et al.* Rapid and highly efficient mammalian cell engineering via Cas9 protein transfection. *Journal of Biotechnology* 2015;**208**:44-53 doi 10.1016/j.jbiotec.2015.04.024.

58. Kim S, Kim D, Cho SW, Kim J, Kim JS. Highly efficient RNA-guided genome editing in human cells via delivery of purified Cas9 ribonucleoproteins. *Genome Research* 2014;**24**(6):1012-9 doi 10.1101/gr.171322.113.

59. Hendel A, Bak RO, Clark JT, Kennedy AB, Ryan DE, Roy S*, et al.* Chemically modified guide RNAs enhance CRISPR-Cas genome editing in human primary cells. *Nature Biotechnology* 2015;**33**(9):985-9 doi 10.1038/nbt.3290.

60. Doench JG, Fusi N, Sullender M, Hegde M, Vaimberg EW, Donovan KF*, et al.* Optimized sgRNA design to maximize activity and minimize off-target effects of CRISPR-Cas9. *Nature Biotechnology* 2016;**34**(2):184-91 doi 10.1038/nbt.3437.

61. Shifrut E, Carnevale J, Tobin V, Roth TL, Woo JM, Bui CT*, et al.* Genome-wide CRISPR Screens in Primary Human T Cells Reveal Key Regulators of Immune Function. *Cell* 2018;**175**(7):1958-71.e15 doi 10.1016/j.cell.2018.10.024.

62. Schmittgen TD, Livak KJ. Analyzing real-time PCR data by the comparative CT method. *Nature Protocols* 2008;**3**(6):1101-8 doi 10.1038/nprot.2008.73.

63. Watson JV, Chambers SH, Smith PJ. A pragmatic approach to the analysis of DNA histograms with a definable G1 peak. *Cytometry* 1987;**8**(1):1-8 doi 10.1002/cyto.990080101.

64. Köbel M, Piskorz AM, Lee S, Lui S, LePage C, Marass F*, et al.* Optimized p53 immunohistochemistry is an accurate predictor of TP53 mutation in ovarian carcinoma. *The Journal of Pathology: Clinical Research* 2016;**2**(4):247-58 doi 10.1002/cjp2.53.

65. Hollis RL, Thomson JP, Stanley B, Churchman M, Meynert AM, Rye T*, et al.* Molecular stratification of endometrioid ovarian carcinoma predicts clinical outcome. *Nature Communications* 2020;**11**(1) doi 10.1038/s41467-020-18819-5.

66. Weinberg RA. The retinoblastoma protein and cell cycle control. *Cell* 1995;**81**(3):323-30 doi 10.1016/0092-8674(95)90385-2.

67. Genovese C, Trani D, Caputi M, Claudio PP. Cell cycle control and beyond: emerging roles for the retinoblastoma gene family. *Oncogene* 2006;**25**(38):5201-9 doi 10.1038/sj.onc.1209652.

68. Findlay GM, Daza RM, Martin B, Zhang MD, Leith AP, Gasperini M*, et al.* Accurate classification of BRCA1 variants with saturation genome editing. *Nature* 2018;**562**(7726):217-22 doi 10.1038/s41586-018-0461-z.

69. Degasperi A, Amarante TD, Czarnecki J, Shooter S, Zou X, Glodzik D*, et al.* A practical framework and online tool for mutational signature analyses show intertissue variation and driver dependencies. *Nature Cancer* 2020;**1**(2):249-63 doi 10.1038/s43018-020-0027-5.

70. Alexandrov LB, Kim J, Haradhvala NJ, Huang MN, Tian Ng AW, Wu Y*, et al.* The repertoire of mutational signatures in human cancer. *Nature* 2020;**578**(7793):94-101 doi 10.1038/s41586-020-1943-3.

71. Kang EY, Weir A, Meagher NS, Farrington K, Nelson GS, Ghatage P*, et al.* CCNE1 and survival of patients with tubo-ovarian high-grade serous carcinoma: An Ovarian Tumor Tissue Analysis consortium study. *Cancer* 2022;**54**(4):538-45 doi 10.1002/cncr.34582.

72. Newman AM, Steen CB, Liu CL, Gentles AJ, Chaudhuri AA, Scherer F*, et al.* Determining cell type abundance and expression from bulk tissues with digital cytometry. *Nature Biotechnology* 2019;**37**(7):773-82 doi 10.1038/s41587-019-0114-2.

73. da Costa AABA, do Canto LM, Larsen SJ, Ribeiro ARG, Stecca CE, Petersen AH*, et al.* Genomic profiling in ovarian cancer retreated with platinum based chemotherapy presented homologous recombination deficiency and copy number imbalances of CCNE1 and RB1 genes. *BMC Cancer* 2019;**19**(1):422- doi 10.1186/s12885-019-5622-4.

74. Hollis RL, Meynert AM, Michie CO, Rye T, Churchman M, Hallas-Potts A*, et al.* Multiomic Characterization of High-Grade Serous Ovarian Carcinoma Enables High-Resolution Patient Stratification. *Clinical Cancer Research* 2022;**28**(16):3546-56 doi 10.1158/1078-0432.CCR-22-0368.

75. Mandigo AC, Tomlins SA, Kelly WK, Knudsen KE. Relevance of pRB Loss in Human Malignancies. *Clin Cancer Res* 2022;**28**(2):255-64 doi 10.1158/1078-0432.CCR-21-1565.

76. de Jonge MM, Auguste A, van Wijk LM, Schouten PC, Meijers M, ter Haar NT*, et al.* Frequent Homologous Recombination Deficiency in High-grade Endometrial Carcinomas. *Clinical Cancer Research* 2019;**25**(3):1087-97 doi 10.1158/1078-0432.CCR-18-1443.

77. Assem H, Rambau PF, Lee S, Ogilvie T, Sienko A, Kelemen LE*, et al.* High-grade Endometrioid Carcinoma of the Ovary. *American Journal of Surgical Pathology* 2018;**42**(4):534-44 doi 10.1097/PAS.0000000000001016.

78. Ku SY, Rosario S, Wang Y, Mu P, Seshadri M, Goodrich ZW*, et al.* Rb1 and Trp53 cooperate to suppress prostate cancer lineage plasticity, metastasis, and antiandrogen resistance. *Science* 2017;**355**(6320):78-83 doi 10.1126/science.aah4199.

79. Mu P, Zhang Z, Benelli M, Karthaus WR, Hoover E, Chen C-C*, et al.* SOX2 promotes lineage plasticity and antiandrogen resistance in TP53 - and RB1 -deficient prostate cancer. *Science* 2017;**355**(6320):84-8 doi 10.1126/science.aah4307.

80. Derenzini M, Donati G, Mazzini G, Montanaro L, Vici M, Ceccarelli C*, et al.* Loss of Retinoblastoma Tumor Suppressor Protein Makes Human Breast Cancer Cells More Sensitive to Antimetabolite Exposure. *Clinical Cancer Research* 2008;**14**(7):2199-209 doi 10.1158/1078-0432.CCR-07-2065.

81. Treré D, Brighenti E, Donati G, Ceccarelli C, Santini D, Taffurelli M*, et al.* High prevalence of retinoblastoma protein loss in triple-negative breast cancers and its association with a good prognosis in patients treated with adjuvant chemotherapy. *Annals of Oncology* 2009;**20**(11):1818-23 doi 10.1093/annonc/mdp209.

82. Patel JM, Goss A, Garber JE, Torous V, Richardson ET, Haviland MJ*, et al.* Retinoblastoma protein expression and its predictors in triple-negative breast cancer. *NPJ breast cancer* 2020;**6**(1):19- doi 10.1038/s41523-020-0160-4.

83. Bowtell DD. The genesis and evolution of high-grade serous ovarian cancer. *Nat Rev Cancer* 2010;**10**(11):803-8 doi nrc2946 [pii]
10.1038/nrc2946.

84. Cancer Genome Atlas N. Comprehensive molecular portraits of human breast tumours. *Nature* 2012;**490**(7418):61-70 doi 10.1038/nature11412.

85. Köbel M, Kalloger SE, Boyd N, McKinney S, Mehl E, Palmer C*, et al.* Ovarian carcinoma subtypes are different diseases: implications for biomarker studies. *PLoS medicine* 2008;**5**(12):e232-e doi 10.1371/journal.pmed.0050232.

86. Miller RE, Leary A, Scott CL, Serra V, Lord CJ, Bowtell D*, et al.* ESMO recommendations on predictive biomarker testing for homologous recombination

deficiency and PARP inhibitor benefit in ovarian cancer. *Annals of Oncology* 2020;**31**(12):1606-22 doi 10.1016/j.annonc.2020.08.2102.

87. Kang EY, Millstein J, Popovic G, Meagher NS, Bolithon A, Talhouk A*, et al.* MCM3 is a novel proliferation marker associated with longer survival for patients with tubo-ovarian high-grade serous carcinoma. *Virchows Archiv* 2022;**480**(4):855-71 doi 10.1007/s00428-021-03232-0.

88. Zhao Y, Wang Y, Zhu F, Zhang J, Ma X, Zhang D. Gene expression profiling revealed MCM3 to be a better marker than Ki67 in prognosis of invasive ductal breast carcinoma patients. *Clinical and Experimental Medicine* 2020;**20**(2):249-59 doi 10.1007/s10238-019-00604-4.

89. Velez-Cruz R, Manickavinayaham S, Biswas AK, Clary RW, Premkumar T, Cole F*, et al.* RB localizes to DNA double-strand breaks and promotes DNA end resection and homologous recombination through the recruitment of BRG1. *Genes Dev* 2016;**30**(22):2500-12 doi 10.1101/gad.288282.116.

90. Westphalen CB, Fine AD, André F, Ganesan S, Heinemann V, Rouleau E*, et al.* Pan-cancer Analysis of Homologous Recombination Repair–associated Gene Alterations and Genome-wide Loss-of-Heterozygosity Score. *Clinical Cancer Research* 2022;**28**(7):1412-21 doi 10.1158/1078-0432.CCR-21-2096.

91. Bruand M, Barras D, Mina M, Ghisoni E, Morotti M, Lanitis E*, et al.* Cell-autonomous inflammation of BRCA1-deficient ovarian cancers drives both tumor-intrinsic immunoreactivity and immune resistance via STING. *Cell Reports* 2021;**36**(3):109412-doi 10.1016/j.celrep.2021.109412.

92. Meng J, Liu X, Zhang P, Li D, Xu S, Zhou Q*, et al.* Rb selectively inhibits innate IFN-β production by enhancing deacetylation of IFN-β promoter through HDAC1 and HDAC8. *Journal of Autoimmunity* 2016;**73**:42-53 doi 10.1016/j.jaut.2016.05.012.

93. Manzano RG, Catalan-Latorre A, Brugarolas A. RB1 and TP53 co-mutations correlate strongly with genomic biomarkers of response to immunity checkpoint inhibitors in urothelial bladder cancer. *BMC Cancer* 2021;**21**(432) doi 10.1186/s12885-021-08078-y.

94. Molinero L, Li Y, Chang C-W, Maund S, Berg M, Harrison J*, et al.* Tumor immune microenvironment and genomic evolution in a patient with metastatic triple negative breast cancer and a complete response to atezolizumab. *Journal for ImmunoTherapy of Cancer* 2019;**7**(274) doi 10.1186/s40425-019-0740-8.

95. Ahmed AA, Etemadmoghadam D, Temple J, Lynch AG, Riad M, Sharma R*, et al.* Driver mutations in TP53 are ubiquitous in high grade serous carcinoma of the ovary. *Journal of Pathology* 2010;**221**(1):49-56 doi 10.1002/path.2696.

96. Landen CN, Molinero L, Hamidi H, Sehouli J, Miller A, Moore KN*, et al.* Influence of Genomic Landscape on Cancer Immunotherapy for Newly Diagnosed Ovarian Cancer: Biomarker Analyses from the IMagyn050 Randomized Clinical Trial. *Clinical Cancer Research* 2023;**29**(9):1698-707 doi 10.1158/1078-0432.CCR-22-2032.

97. Kandalaft LE, Odunsi K, Coukos G. Immune Therapy Opportunities in Ovarian Cancer. *American Society of Clinical Oncology Educational Book* 2020;**3**(40):e228-e40 doi 10.1200/EDBK_280539.

98. Gong X, Du J, Parsons SH, Merzoug FF, Webster Y, Iversen PW*, et al.* Aurora A Kinase Inhibition Is Synthetic Lethal with Loss of the RB1 Tumor Suppressor Gene. *Cancer Discov* 2019;**9**(2):248-63 doi 10.1158/2159-8290.CD-18-0469.

99. Lyu J, Yang EJ, Zhang B, Wu C, Pardeshi L, Shi C*, et al.* Synthetic lethality of RB1 and aurora A is driven by stathmin-mediated disruption of microtubule dynamics. *Nat Commun* 2020;**11**(1):5105 doi 10.1038/s41467-020-18872-0.

100. Oser MG, Fonseca R, Chakraborty AA, Brough R, Spektor A, Jennings RB*, et al.* Cells Lacking the RB1 Tumor Suppressor Gene Are Hyperdependent on Aurora B Kinase for Survival. *Cancer Discov* 2019;**9**(2):230-47 doi 10.1158/2159-8290.CD-18-0389.

101. Serra V, Wang AT, Castroviejo-Bermejo M, Polanska UM, Palafox M, Herencia-Ropero A*, et al.* Identification of a Molecularly-Defined Subset of Breast and Ovarian Cancer Models that Respond to WEE1 or ATR Inhibition, Overcoming PARP Inhibitor Resistance. *Clinical Cancer Research* 2022;**28**(20):4536-50 doi 10.1158/1078-0432.CCR-22-0568.

Table 1. Clinicopathological characteristics and RB1 expression patterns across histotypes

	HGSC		LGSC		MOC		ENOC		CCOC		Total		
	n	(%)	*n*	(%)	*n*	(%)	*n*	(%)	*n*	(%)	*n*	(%)	*P*
Patients													
Number (% of total)	5009	(67)	224	(3)	409	(6)	1033	(14)	761	(10)	7436		
Age at diagnosis (years)													
													<
Median	61		55		56		54		55		59		0.0001[a]
Min-max	21–92		23–88		23–95		21–91		27–89		21–95		
1%-99% percentile	37–84		25–87		24–87		30–84		33–83		32–84		
FIGO stage													
													<
I/II	894	(18)	67	(30)	310	(76)	805	(78)	567	(75)	2643	(36)	0.0001[b]
III/IV	3841	(77)	137	(61)	57	(14)	147	(14)	168	(22)	4350	(58)	
Unknown	274	(5)	20	(9)	42	(10)	81	(8)	26	(3)	443	(6)	
Residual disease													
													<
Absent	1023	(20)	73	(33)	162	(40)	461	(45)	352	(46.3)	2071	(27.9)	0.0001[b]
Present	1488	(30)	52	(23)	21	(5)	41	(4)	78	(10.2)	1680	(22.6)	
Unknown	2498	(50)	99	(44)	226	(55)	531	(51)	331	(43.5)	3685	(49.6)	
RB1 protein													
													<
Loss	734	(15)	5	(2)	7	(2)	37	(4)	12	(2)	795	(11)	0.0001[c]
Retained	3748	(75)	176	(79)	319	(78)	871	(84)	655	(86)	5769	(78)	
Subclonal loss	58	(1)	0	(0)	0	(0)	7	(1)	1	(0)	66	(1)	
Cytoplasmic	13	(0)	0	(0)	1	(0)	1	(0)	2	(0)	17	(0)	
Uninterpretable	456	(9)	43	(19)	82	(20)	117	(11)	91	(12)	789	(11)	

[a]Kruskal-Wallis test and [b]Chi-square test *P* values are reported, excluding cases with 'unknown' information. [c]Chi-square test excluding cases with subclonal loss, cytoplasmic or uninterpretable RB1 protein expression.

HGSC, high-grade serous carcinoma; LGSC, low-grade serous carcinoma; MOC, mucinous ovarian cancer; ENOC, endometrioid ovarian cancer; CCOC, clear cell ovarian cancer.

Table 2. Multivariate analysis of molecular alterations and overall survival in patients with HGSC and ENOC

Histotype	Feature	Category	No. patients	(events, %)	HR	(95% CI)	*P*	P_{int}
HGSC[a,b]								
	RB1							
		Retained	3453	(71.3)	1	[Reference]		
		Loss	686	(61.1)	0.74	(0.66-0.83)	6.8×10^{-7}	
	RB1 and *BRCA* status							
		RB1 retained & g*BRCA*wt	714	(76.3)	1	[Reference]		0.24
		RB1 loss & g*BRCA*wt	135	(60.7)	0.74	(0.57-0.96)	0.023	
		RB1 retained & g*BRCA*var	159	(67.9)	0.69	(0.55-0.86)	0.001	
		RB1 loss & g*BRCA*var	70	(42.9)	0.38	(0.25-0.58)	5.2×10^{-6}	
ENOC[a]								
	RB1							
		Retained	649	(22.7)	1	[Reference]		
		Loss	28	(39.3)	2.17	(1.17-4.03)	0.014	
	RB1 and p53							
		RB1 retained & p53 normal	492	(17.5)	1	[Reference]		0.698
		RB1 retained & p53 abnormal	58	(36.2)	2.26	(1.38-3.71)	0.001	
		RB1 loss & p53 normal	11	(27.3)	1.77	(0.56-5.65)	0.332	
		RB1 loss & p53 abnormal	12	(58.3)	5.34	(2.43-11.8)	<0.001	

[a]Adjusted for stage and age at diagnosis. [b]Stratified by study.

HR, hazard ratio; CI, confidence interval; P_{int}, *P* for interaction; HGSC, high-grade serous carcinoma; ENOC, endometrioid ovarian cancer; g*BRCA*wt, germline *BRCA* wild-type; g*BRCA*var, germline *BRCA* pathogenic variant.

Figure legends:

Figure 1. Expression of RB1 and survival associations across ovarian cancer histotypes.

(A) Representative images of immunohistochemical detection of RB1 expression in ovarian carcinoma tissues, showing examples of the three most common expression patterns: retained, lost and subclonal loss. (B) Proportion of patients with loss or retention of RB1 protein expression in tumor samples by ovarian cancer histotypes. Chi-square *P* value reported for difference in proportions across all histotypes. HGSC, tubo-ovarian high-grade serous carcinoma; LGSC, low-grade serous carcinoma; MOC, mucinous ovarian cancer; ENOC, endometrioid ovarian cancer; CCOC, clear cell ovarian cancer. (C) Boxplots show *RB1* mRNA expression (NanoString) by RB1 protein expression status; lines indicate median and whiskers show range (Mann-Whitney test *P* value reported). Kaplan-Meier analysis of overall survival in patients diagnosed with HGSC (D) and ENOC (E) stratified by tumor RB1 expression. (F) Frequency of germline *BRCA* wild-type (g*BRCA*wt) and germline *BRCA* pathogenic variants (g*BRCA*var) in patients with HGSC stratified by RB1 protein expression. Chi-square *P* value is reported. (G) Kaplan-Meier estimates of overall survival in patients with HGSC by combined germline *BRCA* and tumor RB1 expression status.

Figure 2. Sensitivity to therapeutic agents in *BRCA1*-altered cell lines with *RB1* knockout.

(A) *RB1* was knocked out using CRISPR/Cas9 in 3 patient-derived Australian Ovarian Cancer Study (AOCS) HGSC cell lines with either wild-type or altered *BRCA1* (*BRCA1* var) background. Representative Western Blots show protein levels of RB1 and phosphorylated RB1 (pRB1) compared to GAPDH loading control in single cell cloned, homozygous *RB1* wildtype (WT) and knockout (KO) colonies in comparison to heterogeneous populations with a scramble single guide RNA (sgRNA). Independent blots were used for RB1 and pRB1. (B)

Cell viability was compared between *RB1* WT and KO clones following treatment with cisplatin (72 hours), paclitaxel (72 hours) or olaparib (120 hours). Nonlinear regression drug curves are shown; *P* values are shown in Supplementary Table S18 (n = 3). Error bars indicate ± SEM; for some values error bars are shorter than the symbols and thus are not visible. (C) Proportion of surviving colonies following 16 days of treatment with cisplatin, paclitaxel or a combination of both (with half of the IC50 determined per drug and cell line respectively) relative to DMF vehicle control (n = 3 replicates). Data are presented as mean ± SEM. Mean values were compared by student's t-test (ns, not significant; *P < 0.05; **P < 0.01). Representative scans of the fixed cell colonies stained with crystal violet are shown for each condition.

Figure 3. Genomic landscape of high-grade serous ovarian tumors with co-occurring *BRCA* and *RB1* alterations.

(A) Pathogenic germline and somatic alterations in homologous recombination (HR) and DNA repair genes detected by whole-genome sequencing and DNA methylation analysis of 126 primary HGSC samples (27) are shown, as well as alterations in immune genes and *CCNE1*. Samples are grouped by HR and *RB1* status (HRD, homologous recombination deficient; HRP, homologous recombination proficient). Bars at the top indicate the number of alterations in each listed gene per patient. Patients are annotated with survival group (LTS, long-term survivor, OS >10 years; MTS, mid-term survivor, OS 2-10 years; STS, short-term survivor, OS <2 years), tumor CHORD(41) scores, and the proportion of structural variant (SV) type (DUP, duplication; DEL, deletion; INV, inversion; ITX, intra-chromosomal translocation). (B) Kaplan-Meier estimates of progression-free and overall survival of patients according to HR status (*BRCA1*-type HRD, *BRCA2*-type HRD or HRP tumors) and *RB1* status (altered versus wild-type).

Figure 4. Characterization of HGSC with co-loss of RB1 and *BRCA*.

(A) Gene set enrichment analysis indicating up- and downregulated pathways in tumors according to *BRCA* and *RB1* status. HRP, homologous recombination proficient; HRD, homologous recombination deficient; RB1-wt, *RB1* wild-type; RB1-alt, *RB1* altered. (B) Boxplots comparing GSVA pathway enrichment scores of the cGAS-STING and Toll-like receptor signaling pathways between molecular subgroups; points represent each sample, boxes show the interquartile range (25-75th percentiles), central lines indicate the median, and whiskers show the smallest/largest values within 1.5 times the interquartile range. Colored boxes with black points indicate the HRD and/or *RB1* altered groups whereas the grey boxes with grey points indicate the HRP and *RB1* wild-type group. *P* values were calculated using a two-sided Mann-Whitney-Wilcoxon test. Benjamini-Hochberg adjusted *P* values are shown above each pairwise comparison (*$P < 0.05$, **$P < 0.01$, ns $P \geq 0.05$). (C) Bubble plot summary of *HLA* gene expression comparisons using DESeq2 between HGSC tumors grouped by HRD and/or *RB1* status as shown. The size of the bubbles corresponds to the negative $\log_{10}$ Benjamini-Hochberg adjusted *P* value (P_{adj}) and only values with $P_{adj} \leq 0.1$ are shown. The color and intensity correspond to the $\log_2$ fold-change. Genes are grouped by their classes. (D) Proportion of tumor infiltrating lymphocytes (TILs) in HGSC tumors grouped by RB1 protein expression and *BRCA* germline status. g*BRCA*wt, germline *BRCA* wild-type; g*BRCA*var, germline *BRCA* pathogenic variant. Chi-square *P* value is indicated. (E) Proportion of tumors classified as each HGSC molecular subtype (13) grouped by RB1 expression and *BRCA* germline status. Chi-square *P* value is indicated. C5.PRO, C5/proliferative subtype; C4.DIF, C4/differentiated subtype; C2.IMM, C2/immunoreactive subtype; C1.MES, C1/mesenchymal subtype.

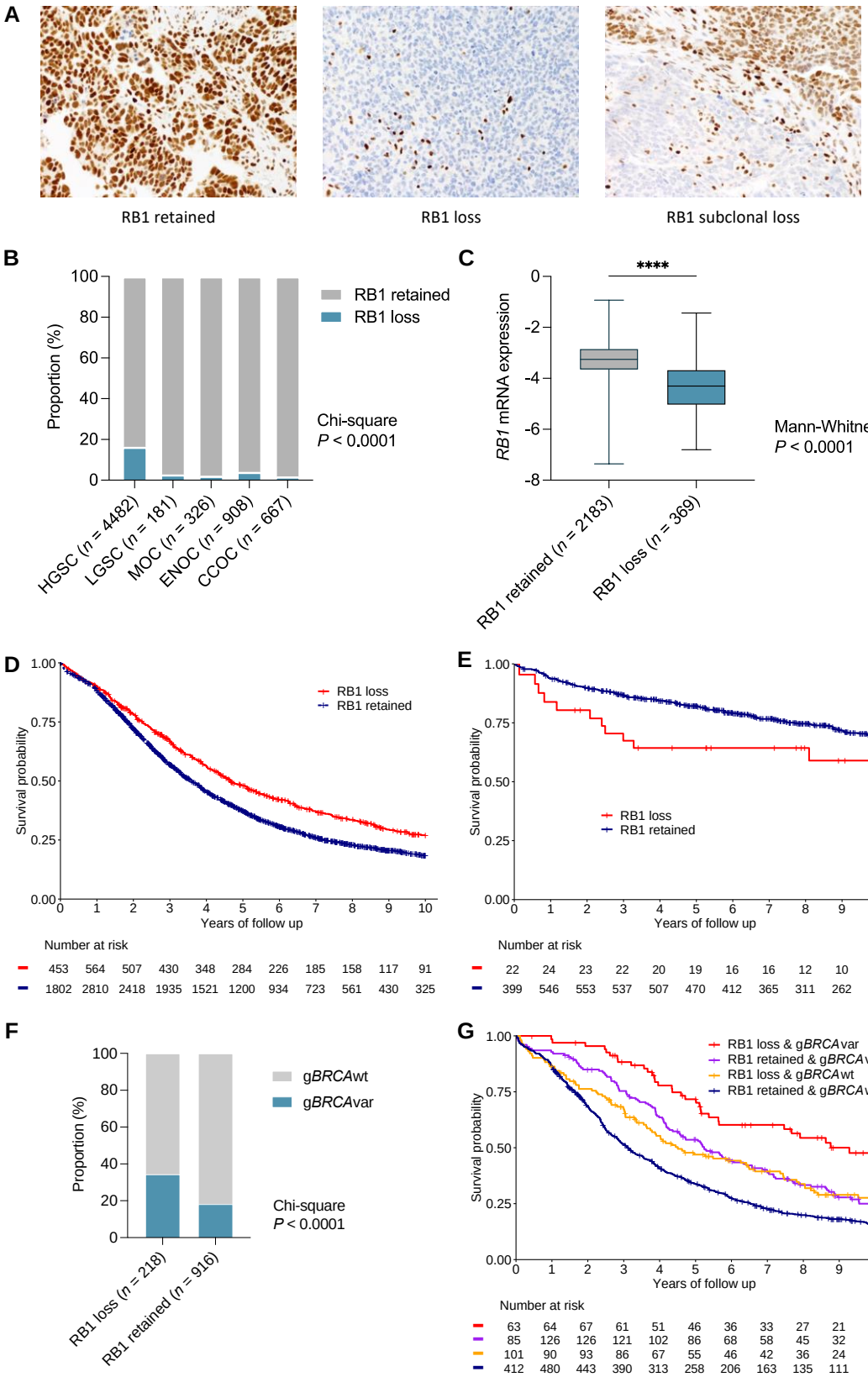

Figure 1.

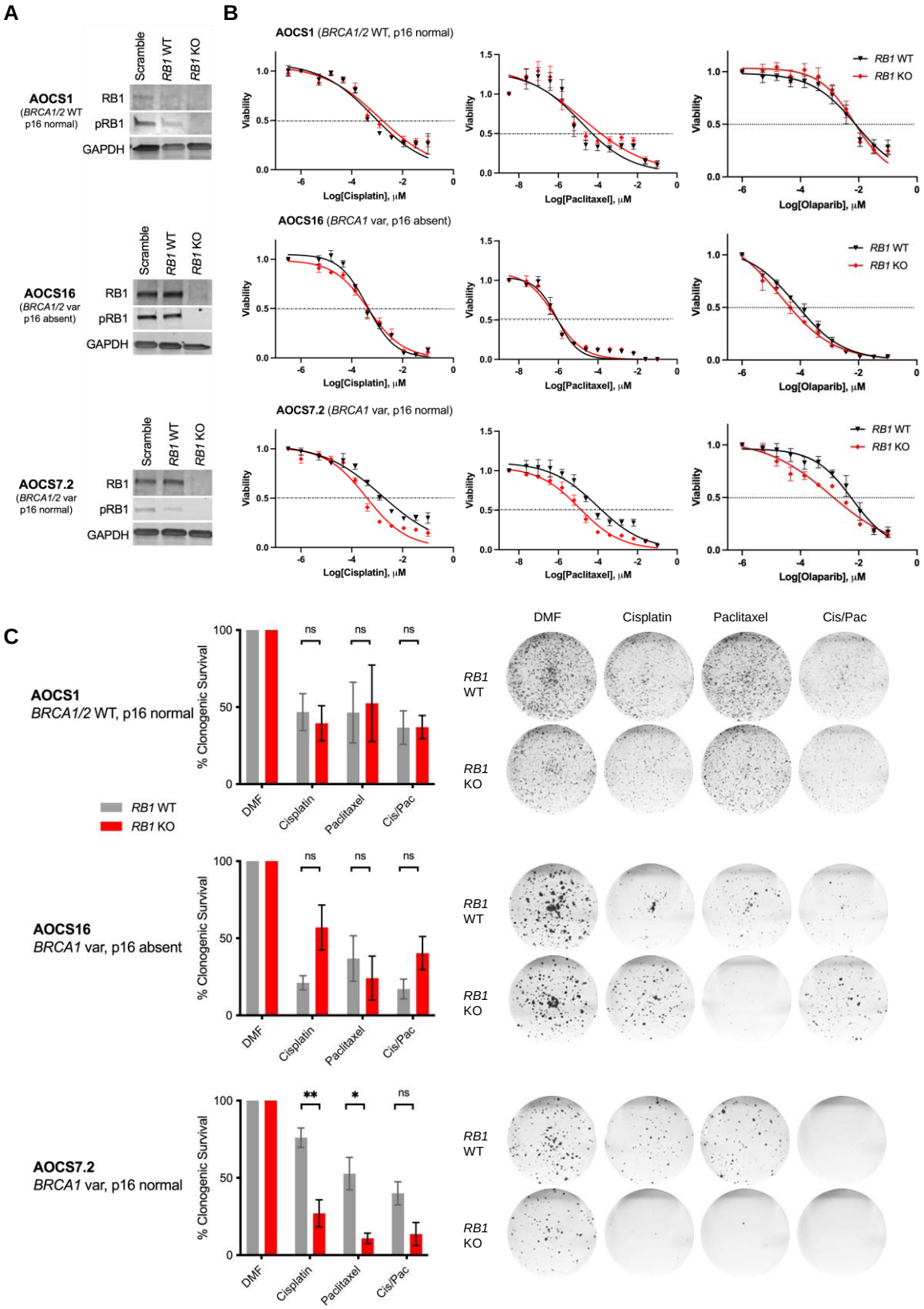

Figure 2.

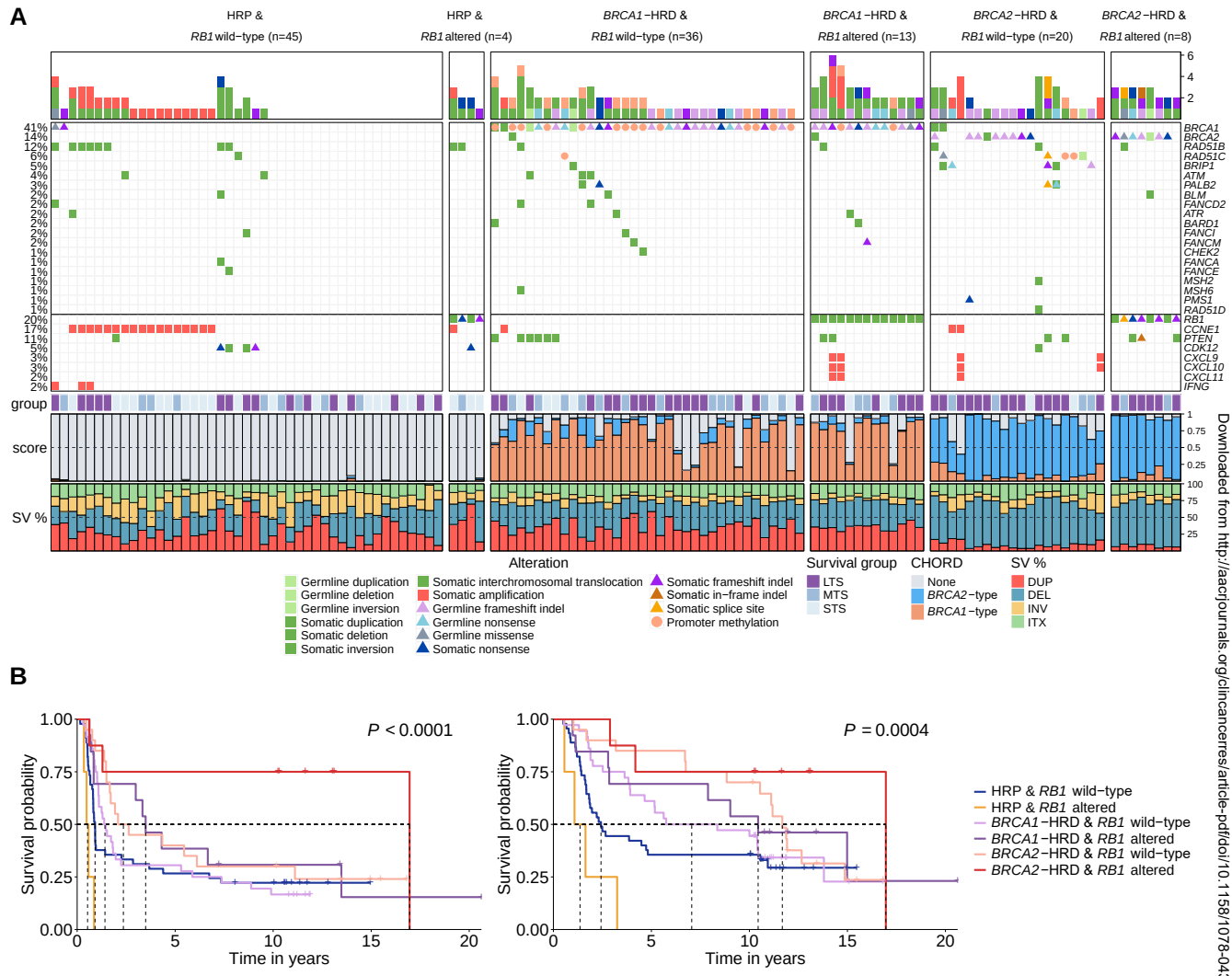

Figure 3.

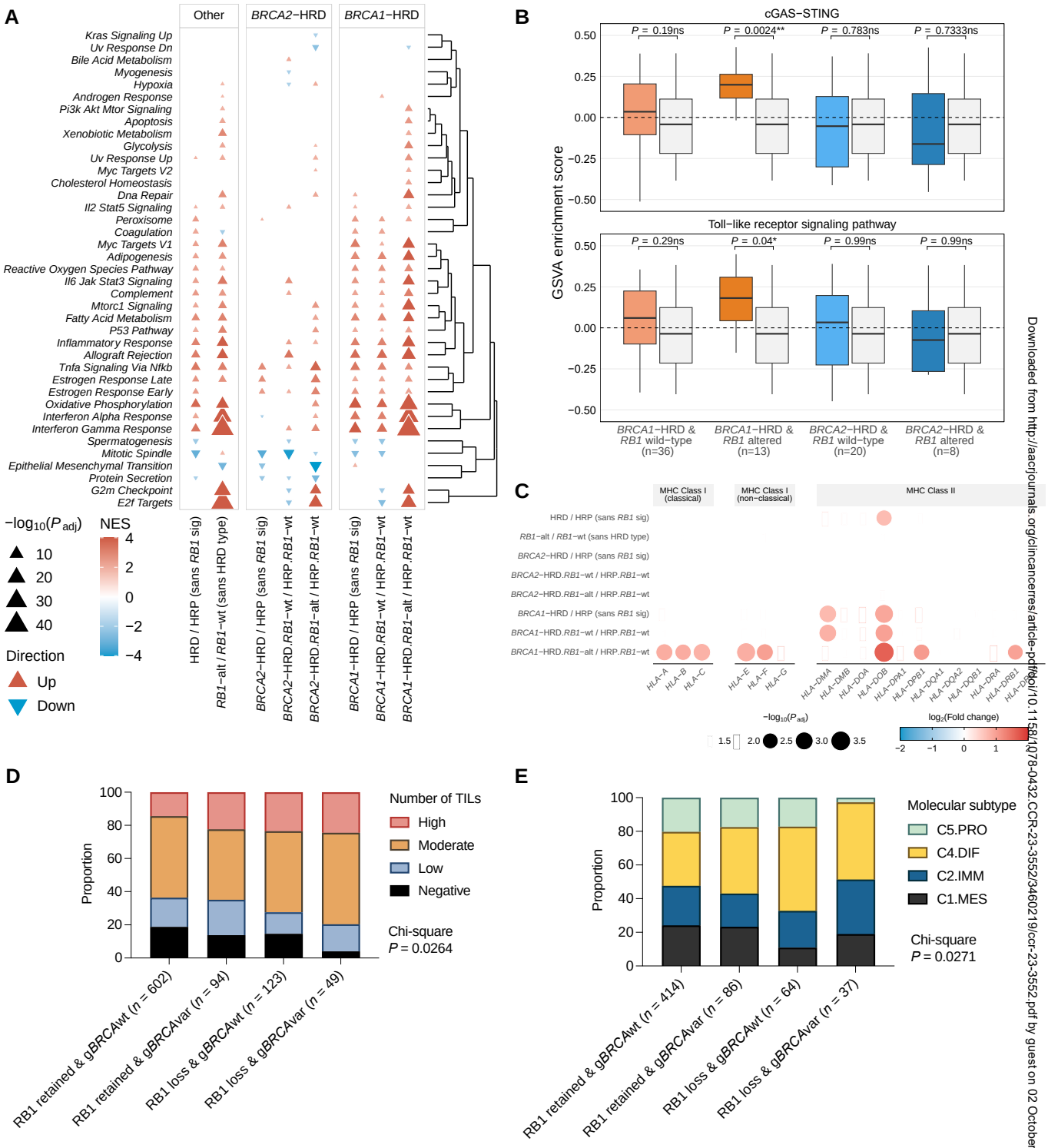

Figure 4.